

000 001 002 003 004 005 006 007 008 009 010 011 012 013 014 015 016 017 018 019 020 021 022 023 024 025 026 027 028 029 030 031 032 033 034 035 036 037 038 039 040 041 042 043 044 045 046 047 048 049 050 051 052 053 DOUBLY-ROBUST LLM-AS-A-JUDGE: EXTERNALLY VALID ESTIMATION WITH IMPERFECT PERSONAS

Anonymous authors
Paper under double-blind review

ABSTRACT

As Generative AI (GenAI) systems see growing adoption, a key concern involves the *external validity* of evaluations, or the extent to which they generalize from lab-based to real-world deployment conditions. Threats to the external validity of GenAI evaluations arise when the source sample of human raters and system outputs used to obtain a system quality estimate differs from the target distribution at deployment time. In this work, we propose a *doubly-robust* estimation framework designed to address this evaluation sampling bias. Key to our approach is the use of “persona” ratings produced by prompting an LLM evaluator (i.e., an LLM-as-a-judge) to behave as a human rater with specific sociodemographic characteristics. Our doubly-robust framework combines these informative yet imperfect persona ratings with human ratings obtained under evaluation sampling bias to produce statistically valid system quality estimates. In particular, we show that our approach yields valid system quality estimates when *either* (i) a model trained to predict human ratings using persona ratings and source data observed under sampling bias, *or* (ii) a reweighting model that corrects for sampling bias is of sufficient quality. We validate our framework theoretically and via a novel Persona Simulation Framework (PSF) designed to systematically manipulate persona quality and the degree of evaluation sampling bias present in source data. Our work provides a principled foundation for combining imperfect persona ratings with human ratings observed under sampling bias to obtain valid system quality estimates.

1 INTRODUCTION

As Generative AI (GenAI) systems see growing adoption, a key concern involves the *external validity* of evaluations, or the extent to which they generalize from lab-based to real-world deployment conditions (Ibrahim et al., 2024; Ouyang et al., 2023; Liao & Xiao, 2023; Liao et al., 2021; Weidinger et al., 2025). In particular, many evaluations report a *system quality estimate*, which reflects the proportion of outputs rated to exhibit a capability (e.g., “helpfulness”) or defect (e.g., “toxicity”) by a human with specialized characteristics (e.g., domain knowledge, cultural experience). However, such quality estimates may fail to generalize when the *source* distribution of human raters and system outputs available at evaluation time differs from the *target* distribution encountered upon deployment. For example, in medical visit summarization, covariate shift arises when we wish to obtain a system quality estimate via expert physician ratings, but [collect supplementary medical student ratings to augment evaluation data](#) (Cai et al., 2022). Selection bias may also occur if medical students rate complex summaries [less often](#) than more experienced physicians. Left unaddressed, these forms of *evaluation sampling bias* threaten the external validity of system quality estimates.

Recent work has proposed tools for improving system quality estimates when human ratings are scarce but black-box predictions (e.g., from an LLM-as-a-judge) are cheap and abundant (Chatzi et al., 2024; Fisch et al., 2024; Eyre & Madras, 2024; Dorner et al., 2024; Saad-Falcon et al., 2023; Fogliato et al., 2024). For instance, Prediction Powered Inference (PPI) offers an approach for leveraging a subset of labeled (source) data to correct for bias in black-box model predictions (Angelopoulos et al., 2023a;b). This bias correction enables using black-box predictions generated over unlabeled (target) samples to shrink confidence intervals around quality estimates while

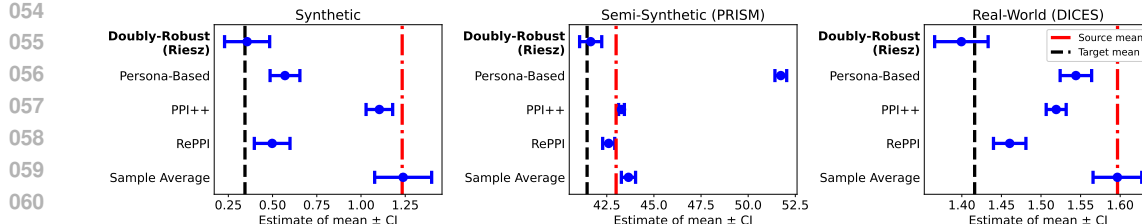


Figure 1: Comparison of our doubly-robust estimator with baselines on three datasets from our Persona Simulation Framework. Red and black dashed lines denote the true source and target mean ratings, respectively (e.g., the average “helpfulness” rating obtained over source vs. target distributions).

Persona-Based directly leverages persona ratings to compute system quality estimates. *Sample Average* produces a system quality estimate by averaging ratings sampled from the source distribution. *PPI++* (Angelopoulos et al., 2023b) and *RePPI* (Ji et al., 2025) are two state-of-the-art statistical methods that do not account for evaluation sampling bias. Across settings, we observe that our Doubly-Robust (Riesz) approach yields improved coverage and lower bias than baselines, while maintaining informative confidence intervals.

maintaining valid coverage. However, both PPI and its extensions (e.g., PPI++ (Angelopoulos et al., 2023b), RePPI (Ji et al., 2025)) assume that (i) source and target samples are drawn i.i.d. and (ii) labels are *missing completely at random* (MCAR) (Tsiatis, 2006), i.e. that successful completion of a rating is independent of rater and text characteristics. However, when source data is observed under sampling bias, these assumptions are violated and severe miscoverage occurs (see Fig. 1).

In this work, we devise an estimator that directly corrects for evaluation sampling bias. Like existing approaches (Angelopoulos et al., 2023b; Ji et al., 2025), our proposal leverages black-box predictions generated by a GenAI system over unlabeled (target) samples to improve statistical inference. Unlike existing estimators, however, our proposal is *doubly-robust* (Bang & Robins, 2005; Chernozhukov et al., 2018): it yields valid system quality estimates if *either* a model trained to predict human ratings from source samples *or* a reweighting model that corrects for sampling bias is of sufficient quality. To attain this doubly-robust property, we leverage *persona ratings* — scores generated by prompting an LLM-as-a-judge to behave as a human rater with desired characteristics (e.g., demographics, expertise) — to learn a high-quality predictor for human ratings from labeled source data. This novel perspective treats persona ratings as an **informative yet imperfect proxy for human ratings** to enhance the quality of downstream system quality estimates.

Figure 1 illustrates the benefits of our estimation approach on three datasets. Whereas directly adopting persona ratings for estimation (Persona-Based) and state-of-the-art baselines (Angelopoulos et al., 2023b; Ji et al., 2025) fail to provide coverage, our approach provides valid confidence intervals, **while also demonstrating low statistical bias. These specific results are indicative of our general findings across experimental conditions, reported in Section 4.** This valid coverage enables practitioners to make reliable deployment decisions; for example, by more confidently determining whether a system’s mean “helpfulness” rating meets deployment standards. To summarize, our main contributions are as follows:

- **We formalize the problem** of GenAI system quality estimation under evaluation sampling bias. Unlike existing statistical frameworks (Angelopoulos et al., 2023b; Ji et al., 2025), our formulation explicitly accounts for both covariate shift and selection bias in observed source ratings to improve the external validity of system quality estimates.
- **We devise a doubly-robust estimator** for GenAI system quality estimation under evaluation sampling bias. En route, we first advance doubly-robust estimation theory by generalizing the work of (Chernozhukov et al., 2023) to M-estimation settings with surrogate (persona) ratings. This generalization enables us to (i) leverage persona ratings to improve doubly-robust system quality estimates, (ii) estimate a richer set of system quality parameters (e.g., rating variance, quantiles) beyond means, and (iii) maintain valid coverage even in the presence of evaluation sampling bias, all desiderata not satisfied by previous works.
- **We advance the practical application of doubly-robust estimators** to GenAI system quality estimation. Whereas doubly-robust estimators are traditionally applied on small tabular datasets, GenAI system quality estimation requires learning a reweighting function over high dimensional (e.g., text, audio) input-output spaces. We show that sentence

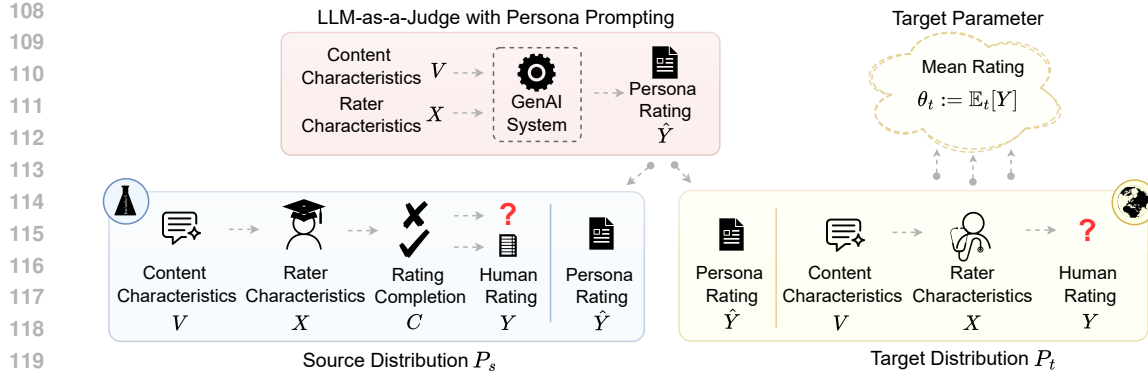


Figure 2: Our framework produces estimates for the target parameter θ_t using (i) complete rating tuples from the source distribution (blue, left), (ii) unlabeled samples from the target distribution (yellow, right), and (iii) persona ratings produced for both source and target samples (red, top). *Evaluation sampling bias* may arise both from the *covariate shift* of (V, X) from P_s to P_t , and from *selection bias* in which rating completion C is non-random in P_s – i.e., $C \not\perp (V, X)$.

transformer embedding models and a “Riesz loss” approach (Chernozhukov et al., 2022b) can be combined to correct for covariate shift in high-dimensional text input-output spaces.

- **We introduce a Persona Simulation Framework (PSF)** that systematically manipulates evaluation sampling bias and persona quality over three datasets encompassing synthetic, semi-synthetic (PRISM) (Kirk et al., 2024), and real-world (DICES) (Aroyo et al., 2023) settings. Leveraging the PSF, we show our estimator obtains valid coverage up to a larger magnitude of sampling bias than state-of-the-art baselines (e.g., RePPI (Ji et al., 2025)).

2 PRELIMINARIES

We provide an overview of the data generating processes and GenAI system quality parameters considered hereinafter. We provide detailed coverage of all notation and assumptions in Appendix B.

Probabilistic Framework. As illustrated in Fig. 2, we model system quality estimation under evaluation sampling bias via a tuple of random variables $Z = (X, V, C, Y, \hat{Y})$. Here, X denotes *rater characteristics* (e.g., age, gender, geographic locale) and V denotes the *content to be rated*, such as the GenAI system input and output. In experiments, we characterize the content V via an embedding-based projection of the input prompt and system output into a low-dimensional space (see § 4). We use $W = (X, V)$ to denote the tuple of rater and content. C is an indicator of rating completion ($C = 1$ if the rater provides a rating, $C = 0$ otherwise). For example, a rater can fail to provide a rating if they (i) are excluded on the basis of failed attention checks, or (ii) abandon the rating task mid-way (i.e., self-attrition). Let Y denote the rating a rater *would* assign if they completed the task ($C = 1$), which may be ordinal (e.g., Likert 1–5), interval (e.g., 1–100), or binary (e.g., Yes/No). Finally, \hat{Y} is the rating returned by an LLM-as-a-judge with persona prompting.

Example 1. Suppose we want to measure the “factual consistency” of medical visit summarization model outputs. Here, X captures raters’ expertise (medical student vs. physician) and V includes the full visit notes and corresponding summary. Rating completion (C) denotes whether the rater successfully provides a rating when prompted, and Y is the human’s “factual consistency” rating (e.g., on a binary scale). Finally, \hat{Y} denotes GPT-4’s predicted rating.

Evaluation Sampling Bias. To model evaluation sampling bias, we assume there are two *full-data* distributions over tuples Z : a source distribution P_s and a target distribution P_t . *Covariate shift* arises when the marginal distribution of rater and content characteristics differs across source and target—i.e., $P_s(W) \neq P_t(W)$. For example, the source distribution may consist of urban clinic summaries rated by medical students, while the target distribution consists of rural clinic summaries rated by physicians. *Selection bias* arises when rating completion depends on rater and/or content characteristics — i.e., $C \not\perp W$. In our running example, this can arise if less experienced medical students are less likely to complete complex summaries than physicians. While our framework is ex-

162
 163
 164
 165
 166
 167 Table 1: Examples of statistical parameters recovered by our M-estimation framework. Each parameter summarizes information about human ratings obtained over the target distribution. Conditional parameters (bottom three rows) can be defined conditionally on rater characteristics (X), content characteristics (V), or both, as special cases of conditioning on $W = (X, V)$.
 168
 169
 170
 171
 172
 173
 174
 175
 176
 177
 178
 179

Parameter	Estimand	Example
Mean	$\theta_t := \mathbb{E}_t[Y]$	Mean “helpfulness” rating for customer service chatbot responses.
Variance	$\theta_t := \text{Var}_t(Y)$	Variance (disagreement) in “code correctness” ratings in the target distribution.
Quantile	$\theta_t := \inf\{y : P_t(Y \leq y) \geq Q\}$	Median “comprehensibility” score for technical documentation.
Conditional Mean	$\theta_t := \mathbb{E}_t[Y \mid g(W) = 1]$	Mean “coherence” rating assigned by <i>domain experts</i> to multi-turn conversational responses.
Conditional Variance	$\theta_t := \text{Var}_t[Y \mid g(W) = 1]$	Variance in “helpfulness” ratings among <i>novice programmers</i> for code suggestions.
Conditional Quantile	$\theta_t := \inf\{y : P_t(Y \leq y \mid g(W) = 1) \geq Q\}$	90th percentile “safety” rating for <i>high-risk queries</i> flagged by content moderators.

180
 181 plicitly designed to handle selection bias, existing frameworks (Angelopoulos et al., 2023b; Ji et al.,
 182 2025) assume that data are missing completely at random (MCAR) — i.e., $C \perp\!\!\!\perp W$. We show em-
 183 pirically that violations of this assumption lead to severe degradation in quality estimates (see § 4).
 184

185 While we relax this MCAR assumption, we rely on several additional assumptions (*also* required by
 186 existing frameworks). For instance, we assume no *concept drift*, i.e., that $P_s(Y|W) = P_t(Y|W)$.
 187 This requires that the rater and content characteristics are sufficiently rich as to describe ratings
 188 across both populations. We elaborate on this and other standard causal assumptions required by our
 189 framework in Appendix B. Relaxing these assumptions remains a fruitful direction for future work.
 190

191 **Estimation Goal.** Given a sample of N_s *partial* source observations $\mathcal{D}_s = \{(X_j^s, V_j^s, C_j^s, C_j^s \cdot$
 192 $Y_j^s, \hat{Y}_j^s\}_{j=1}^{N_s}$ and N_t *partial* target observations $\mathcal{D}_t = \{(X_i^t, V_i^t, \hat{Y}_i^t\}_{i=1}^{N_t}$, our goal is to estimate a
 193 parameter summarizing system quality over P_t .¹² As our running example in the main text and ex-
 194 periments, we consider the mean rating, $\theta_t := \mathbb{E}_t[Y]$, which describes the average “helpfulness” or
 195 “factual consistency” rating assigned by human raters to system outputs in the target distribution P_t .
 196

3 METHODOLOGY

197 We now introduce our doubly-robust estimator for GenAI system quality estimation under evalua-
 198 tion sampling bias. The central challenge addressed by our approach is that our data is imperfect.
 199 While persona predictions are available, they may be a poor proxy for human ratings. Likewise,
 200 human ratings from the source distribution may suffer from evaluation sampling bias, leading to
 201 invalid estimates for the target parameter. We first introduce several naive approaches which might
 202 be used to tackle this problem (§ 3.1). Then, we show that while each approach is insufficient in iso-
 203 lation, they can be combined to obtain valid coverage. (§ 3.2). Our results presented in this section
 204 apply not only when $\theta_t := \mathbb{E}_t[Y]$ (where they generalize Chernozhukov et al. (2023) to simulta-
 205 neous covariate shift *and* selection bias) but also when θ_t is the solution to a generic M-estimation
 206 problem. Table 1 illustrates the range of statistical parameters our framework supports.
 207

3.1 BASELINE APPROACHES AND THEIR LIMITATIONS

208 **Persona-Augmented Regression.** One seemingly reasonable estimation strategy is to train a
 209 model to predict human ratings using source data and then use this model to impute missing
 210 target labels. Persona-augmented regression leverages this approach while including persona
 211

212 ¹We use superscripts s, t on random variables to denote source and target membership. We omit these
 213 superscripts where the distribution is clear from context (e.g., $\mathbb{E}_t[Y]$ clearly refers to the target distribution).
 214

215 ²In the tuple \mathcal{D}_s , the shorthand $C_j^s \cdot Y_j^s$ denotes that ratings are only observed when $C_j^s = 1$.
 216

216 ratings as an *additional auxiliary feature* in the regression function. In particular, we train a
 217 model $\hat{\mu}(W, \hat{Y})$ predicting $\mu_0(W) := \mathbb{E}[Y \mid W]^3$ using samples from \mathcal{D}_s and then estimate θ_t as
 218 $\hat{\theta}_t^{\text{reg}} := \frac{1}{N_t} \sum_{i=1}^{N_t} \hat{\mu}(W_i^t, \hat{Y}_i^t)$. Observe that this persona-augmented regression estimator relies not
 219 only on covariates, but also on the persona rating. While this approach may be viable when persona
 220 ratings are highly correlated with human ratings, in general $\hat{\mu}$ will converge too slowly to construct
 221 valid confidence intervals (§ 4).
 222

223 **Re-weighting.** Another approach is to disregard the persona ratings. One instead might *re-weight*
 224 samples from P_s based on their probability of occurring under P_t . This approach requires correcting
 225 for covariate shift and selection bias in parallel. Formally, let $\omega_0(w) = \frac{dP_t}{dP_s}(w)$ denote the density
 226 ratio between $P_t(W)$ and $P_s(W)$, and let $\pi_0(w) = \mathbb{P}_s(C = 1 \mid W = w)$ denote the probability of
 227 rating completion. Under standard assumptions (see Appendix B), we have $\theta_t = \mathbb{E}_s[\alpha_0(W, C)Y]$,
 228 where $\alpha_0(W, C) := C \frac{\omega_0(W)}{\pi_0(W)}$. Thus, if one produces an ML estimate $\hat{\alpha}$ of α_0 (say by training models
 229 $\hat{\omega}, \hat{\pi}$ predicting ω_0, π_0), they can compute an inverse propensity weighted (IPW) estimate $\hat{\theta}_t^{\text{ipw}} :=$
 230 $\frac{1}{N_s} \sum_{j=1}^{N_s} \hat{\alpha}(W_j^s, C_j^s) \cdot Y_j^s$. Again, estimates of α_0 must converge at parametric rates in order to
 231 maintain coverage. Further, IPW suffers from high variance when propensities are small — a salient
 232 challenge when estimating system quality parameters over high-dimensional (e.g., text) data (§ 4).
 233

234 3.2 DOUBLY-ROBUST ESTIMATOR

235 Our doubly-robust estimator can be viewed as carefully combining the persona-augmented regression
 236 estimator (μ_0) with the re-weighting estimator (α_0). The functions μ_0 and α_0 are referred to as
 237 *nuisance functions* because they are used as an auxiliary information source to estimate the target
 238 statistical parameter of interest θ_t . Our estimator combines these nuisance functions in the form:
 239

$$240 \quad \hat{\theta} = \frac{1}{N_t} \sum_{i=1}^{N_t} \hat{\mu}(W_i^t, \hat{Y}_i^t) + \frac{1}{N_s} \sum_{j=1}^{N_s} \hat{\alpha}(W_j^s, C_j^s) \left\{ Y_j^s - \hat{\mu}(W_j^s, \hat{Y}_j^s) \right\}, \quad (1)$$

241 where $\hat{\mu}$ and $\hat{\alpha}$ are estimates of μ_0 and α_0 that are assumed to be independent of the data. In
 242 Equation (1), the left term evaluates the regression-based estimator over samples from the target distribution.
 243 Analogously to PPI++ (Angelopoulos et al., 2023b), this has the effect of using unlabeled
 244 data to reduce variance in the estimate. The right term corrects for bias in the human rating predictor
 245 $\hat{\mu}$ by re-weighting residualized source data to account for covariate shift and selection bias. This
 246 correction adjusts for bias in persona ratings via the residual term, while correcting for evaluation
 247 sampling bias via the re-weighting function α .
 248

249 To construct confidence intervals, we also consider the variance estimate:
 250

$$251 \quad \hat{\sigma}^2 = \frac{1}{N_t} \sum_{i=1}^{N_t} \left\{ \hat{\mu}(W_i^t, \hat{Y}_i^t) - \hat{m}_t \right\}^2 + \frac{\hat{\gamma}}{N_s} \sum_{j=1}^{N_s} \hat{\alpha}(W_j^s, C_j^s)^2 \left\{ Y_j^s - \hat{\mu}(W_j^s, \hat{Y}_j^s) \right\}^2, \quad (2)$$

252 where $\hat{m}_t = \frac{1}{N_t} \sum_{i=1}^{N_t} \hat{\mu}(W_i^t, \hat{Y}_i^t)$ and $\hat{\gamma}$ is a scaling parameter (described in Algorithm 1). Since
 253 our mean and variance estimators require nuisance estimates that are independent of the data, we use
 254 K -fold cross-fitting to maximize efficiency (Chernozhukov et al., 2018). For each $k \leq K$, we train
 255 nuisance models on all data excluding the samples in fold k . We then use our nuisance estimates to
 256 produce a de-biased parameter estimate for the data in fold k . We then average the per-fold parameter
 257 and variance estimates to maintain full data efficiency. See Algorithms 1 and 2 for full details.
 258

259 Our main result establishes the asymptotic normality of our estimator. Further, it describes how to
 260 build confidence intervals using the mean and variance estimates recovered from Algorithm 1.
 261

262 **Theorem 3.1.** *Assume the learner has access to samples $Z_1^s, \dots, Z_{N_s}^s \sim P_s$ and $Z_1^t, \dots, Z_{N_t}^t \sim P_t$
 263 satisfying Assumptions 1- 2 and the assumptions of Theorems B.2 and B.4, all outlined in Appendix B. Then, letting $\hat{\theta}$ and $\hat{\sigma}^2$ denote the mean and variance returned by Algorithm 1, we have*

$$264 \quad \hat{\sigma}^{-1} \sqrt{N_t} (\hat{\theta} - \theta) \Rightarrow \mathcal{N}(0, 1).$$

265 ³No concept drift implies $\mathbb{E}_t[Y \mid W] = \mathbb{E}_s[Y \mid W]$, so we can omit subscripts without any worry.

270 **Algorithm 1** Doubly-Robust Estimator with K -fold Cross-Fitting

271 1: **Input:** Samples $\mathcal{D}_s = \{Z_1^s, \dots, Z_{N_s}^s\}$ from P_s , samples $\mathcal{D}_t = \{Z_1^t, \dots, Z_{N_t}^t\}$ from P_t , number
272 of folds K .
273 2: Randomly split source indices $[N_s]$ random folds of equal size: $\mathcal{I}_1, \dots, \mathcal{I}_K$.
274 3: **for** $k \in [K]$ **do**
275 4: Produce ML estimate $\hat{\mu}^{(-k)}$ using $\mathcal{D}_{s,k}^c := \mathcal{D}_s \setminus \mathcal{D}_{s,k}$, where $\mathcal{D}_{s,k} := (Z_j^s : j \in \mathcal{I}_k)$.
276 5: Produce ML estimate $\hat{\alpha}^{(-k)}$ using $\mathcal{D}_{s,k}^c$ and \mathcal{D}_t .
277 6: Construct $\hat{\theta}_k$ per Equation (1) with $\hat{\mu} := \hat{\mu}^{(-k)}$, $\hat{\alpha} := \hat{\alpha}^{(-k)}$, and samples $\mathcal{D}_{s,k}$ and \mathcal{D}_t .
278 7: Construct $\hat{\sigma}_k$ per Equation (2) with $\hat{\mu} := \hat{\mu}^{(-k)}$, $\hat{\alpha} := \hat{\alpha}^{(-k)}$, $\hat{\gamma} := \frac{N_t}{N_s}$, and samples $\mathcal{D}_{s,k}$
279 and \mathcal{D}_t .
280 8: Compute the average of the K estimates: $\hat{\theta} := \frac{1}{K} \sum_{k=1}^K \hat{\theta}_k$ and $\hat{\sigma}^2 := \frac{1}{K} \sum_{k=1}^K \hat{\sigma}_k^2$.
281 9: **Return:** Mean estimate $\hat{\theta}$ and variance estimate $\hat{\sigma}^2$.

284
285 *In particular, this implies that, for any $\delta \in (0, 1)$, the set*

286

$$287 C_{1-\delta} := \left[\hat{\theta} - \frac{\hat{\sigma}}{\sqrt{N_t}} z_{\delta/2}, \hat{\theta} + \frac{\hat{\sigma}}{\sqrt{N_t}} z_{\delta/2} \right]$$

288

289 *is a $1 - \delta$ confidence interval for θ , where z_δ denotes the δ quantile of a standard normal R.V.*

290

291 A complete theorem statement can be found in Theorem B.4. In Appendix C, we present a
292 generalization to M-estimators (Theorems C.1 and C.4) and a corresponding proof — the above
293 follows as a special case. We also provide examples of other target parameters, including rating
294 variance and quantiles in Remark C.2 of the same appendix, which may be of independent interest.

295 The validity of Theorem 3.1 relies on several key assumptions, formally outlined in Appendix B. Of
296 these, the most important is *double robustness*, which requires the *product* of nuisance estimation
297 errors to decay at parametric (i.e. $\sqrt{N_t}$) rates. **Formally, this assumption can be expressed via the**
298 **condition that**

299

$$300 \|\hat{\alpha}^{(-k)} - \alpha_0\|_{L^2} \cdot \|\hat{\mu}^{(-k)} - \mu_0\|_{L^2} = o_{\mathbb{P}}(N_t^{-1/2}) \quad (3)$$

301

302 on each fold. See Appendix B for definition of L^2 norms and a formal definition of $o_{\mathbb{P}}$ notation
303 (here, $o_{\mathbb{P}}(N_t^{-\beta})$ denotes convergence in probability at $N_t^{-\beta}$ rates). Notably, this condition allows
304 each individual nuisance estimate to converge at non-parametric rates, thus permitting coverage even
305 when estimates of either α_0 or μ_0 are of lower quality. For instance, one could have

306

$$307 \max \left\{ \|\hat{\mu}^{(-k)} - \mu_0\|_{L^2}, \|\hat{\alpha}^{(-k)} - \alpha_0\|_{L^2} \right\} = o_{\mathbb{P}}(N_t^{-1/4})$$

308

309 and still maintain valid coverage. In other words, when we state that our estimator will provide
310 valid coverage when either *either* (i) a model trained to predict human ratings using persona ratings
311 and source data observed under sampling bias ($\hat{\mu}$), *or* (ii) a reweighting model that corrects for
312 sampling bias ($\hat{\alpha}$) is of sufficient quality, we refer precisely to this product of errors condition (3).

313

314 We also note that the above convergence rate does not *directly* depend on the quality of persona
315 ratings. Rather, the persona ratings serve as an extra covariate onto which we can regress human
316 ratings Y . When persona ratings are highly correlated with human ratings, we may obtain faster
317 convergence rates for $\hat{\mu}$. However, this does not prohibit convergence even when the quality of
318 persona ratings is low. This phenomenon is illustrated in our experiments below.

319

320 **Estimation Details.** In Theorem 3.1 above, estimating μ_0 is a standard regression task that can be
321 accomplished using any off-the-shelf model (e.g. gradient boosted trees, neural networks). How-
322 ever, estimation of $\alpha_0(w, c)$, which is a complicated ratio of likelihood ratios and propensity scores,
323 is more subtle. The standard approach for doubly-robust estimation would involve learning $\hat{\omega}$ and
324 $\hat{\pi}$ separately (e.g., via gradient boosted trees) then estimating $\hat{\alpha}$ by taking the ratio of predictions
325 produced by each model. However, because w can occupy a high dimensional (e.g., text) space, the
326 variance in this ratio can be quite high. This variance in turn propagates to downstream estimates.

327 To address this challenge, we leverage a “Riesz loss” (Chernozhukov et al., 2022b;a; 2023) to es-
328 timate α_0 . Rather than learning ω_0 and π_0 independently, the Riesz loss directly learns the ratio

324 $\alpha_0(w, c)$. For our setting, letting $\beta_0(w) := \omega_0(w)/\pi_0(w)$, the Riesz loss minimizer is given by:
 325

$$\beta_0 = \arg \min_{\beta} \left\{ \mathbb{E}_s[C \cdot \beta(W^s)^2] - 2\mathbb{E}_t[\beta(W^t)] \right\}. \quad (4)$$

328 Therefore, to estimate α_0 , we minimize the finite-sample analogue of Equation 4 using $\mathcal{D}_{s,k}^c$ and
 329 \mathcal{D}_t then plug this into Algorithm 1 (see Appendix D for details). As we show in § 4, this Riesz loss
 330 approach significantly improves the quality of downstream estimates.
 331

332 4 EXPERIMENTS

333 Validating estimators under evaluation sampling bias requires datasets with detailed rater characteristics,
 334 rating completion information, and a mechanism for manipulating the magnitude of bias.
 335 Such datasets are scarce. Even the most extensive datasets (e.g., DICES (Aroyo et al., 2023)) do
 336 not afford control over covariate shift or selection bias. To address this gap, we introduce a *Persona*
 337 *Simulation Framework* (PSF) that provides complete rating tuples $Z = (X, V, C, Y, \hat{Y})$ and allows
 338 us to vary (i) covariate shift, (ii) selection bias, and (iii) persona quality in parallel. The PSF
 339 contains three specific datasets, each of which simulates evaluation data with increasing realism:
 340

- 341 • **Synthetic:** All nuisance functions and target parameters are fully known (see Appendix E).
- 342 • **Semi-Synthetic:** We sample 1000 real user conversations from PRISM (Kirk et al., 2024) and
 343 obtain the “ground truth” target parameter θ_t by treating ratings returned by an LLM-as-a-judge
 344 as human ratings (Y). We sample 50 such LLM ratings per item. Here, true nuisance functions are
 345 unknown. We sample persona ratings \hat{Y} by adding controlled error to the LLM-as-a-judge ratings
 346 (see § 4.1). This dataset instructs raters to assess the “helpfulness” of outputs on a 1-100 scale.
 347
- 348 • **Real-World:** We sample real user conversations, rater characteristics (e.g., age, race), and human
 349 ratings (Y) from DICES (Aroyo et al., 2023), resulting in 300 conversations each with 25 human
 350 ratings each. We then sample persona ratings \hat{Y} by (i) adding controlled error to human ratings
 351 (see § 4.1) and (ii) via an LLM-as-a-judge with persona-based prompting. This dataset instructs
 352 raters to assess the “harmfulness” of outputs on a 1-4 scale.

353 In addition to providing a foundation for validating our doubly-robust estimator, the PSF offers a
 354 resource for the community to test future evaluation approaches under evaluation sampling bias.
 355

356 4.1 DATASET GENERATION PROCEDURE

357 We now describe how semi-synthetic (PRISM) and real-world (DICES) datasets are generated in
 358 the PSF. Further setup details, including prompts used for synthetic dataset generation, are reported
 359 in Appendix E.
 360

361 **Source and Target Populations.** In the semi-synthetic dataset (PRISM), the source population
 362 consists of conversations where users are prompted to engage in controversial topics, while the
 363 target population consists of conversations with no guided prompts. In the real-world dataset
 364 (DICES), the source population contains 350 single-turn conversations flagged by safety experts
 365 as containing a single harm type (e.g., misinformation, legal), while the target contains more
 366 complex conversations rated as containing *multiple* types of harm. In both cases, we model each
 367 sample as a single user–system exchange extracted from a multi-turn dialogue. We embed the
 368 input–output pair from each exchange into a low-dimensional space by first applying an embedding
 369 model (MiniLM-L6-v2) then projecting to 15 dimensions via UMAP (Becht et al., 2019).⁴ We also
 370 vary the demographic composition of raters across populations. In both PRISM and DICES, we
 371 define the source distribution $P_s(X)$ using marginal probabilities of rater characteristics reported
 372 in DICES, and target distribution $P_t(X)$ using population statistics released in the U.S. Census
 373 Bureau’s 2022 Annual Social and Economic Supplement (Guzman & Kollar, 2023).

374 **Covariate Shift.** To vary the magnitude of covariate shift, we control the mixture between the
 375 source and target populations. We vary the content characteristics by controlling the proportion
 376 $\zeta \in [0, 1]$ of target items contained within the source sample (sub-sampling from the full data to
 377

⁴We selected 15 dimensions to ensure embeddings retained some predictive signal for ratings and source/target membership while keeping dimensionality low; results remained stable for ≥ 12 dimensions.

378 ensure that source and target sample sizes remain fixed). Additionally, we vary the rater distributions by taking the convex combination between all groups in each demographic stratum with 379 normalization. The magnitude of the resulting covariate shift between samples is then given by the 380 Sinkhorn Distance $\Delta(W^s, W^t)$ (Feydy et al., 2019), where recall that $W = (X, V)$ and V denotes 381 the embedded content characteristics (MiniLM-L6-v2 + UMAP). We report the Sinkhorn distance 382 normalized by subtracting the baseline case where there is no covariate shift for semi-synthetic 383 and real-world settings, as it is inevitable that there will be variation in text embeddings despite 384 sampling i.i.d. from pre-defined categories (e.g., harm types) within a population. This measure 385 captures covariate shift resulting from content characteristics and demographic attributes in parallel. 386

387 **Selection Bias.** We model *rater attrition*—when raters fail to provide a rating due to failed attention 388 checks or task abandonment—by varying the probability that each item is rated. In PRISM, we 389 prompt the LLM to output both a rating and a non-response “refusal” flag. In DICES, we use rater 390 self-assessments of task understanding to assign attrition scores (see Appendix E). We then 391 transform attrition scores into dropout probabilities using a Beta CDF with $\alpha = 3$ (increasing β increases 392 selection bias). We censor ratings according to these probabilities while retaining the “true” rating. 393 We quantify the magnitude of selection bias via the *dropout rate*, i.e., the probability that a rater 394 fails to rate an item. Crucially, the dropout rates we simulate mirror those observed in practice. In 395 DICES, 19 of 123 raters (15.4%) were excluded due to failed attention checks, while in PRISM, 104 396 of 1500 raters (6.9%) failed to provide ratings after completing the background survey. As we show 397 in our results, existing methods (e.g., RePPI (Ji et al., 2025)) exhibit severe miscoverage at these 398 empirically observed dropout rates. This underscores the importance of correcting for selection bias. 399

400 **Persona Quality.** To systematically manipulate the quality of persona ratings, we perturb human 401 ratings with controlled error. This error perturbation has (i) a bias parameter $\eta \in [-1, 1]$, which 402 induces a systematic shift, and (ii) a correlation parameter $\rho \in [-1, 1]$, which parametrizes the 403 Pearson correlation with human ratings. We construct the persona rating via a Cholesky-based 404 procedure that transforms independent Gaussian noise to achieve the target correlation ρ : 405

$$\hat{Y} = \text{clip}(\rho \cdot Y + \sqrt{1 - \rho^2} \cdot Z\sigma_Y + \eta(y_{\max} - y_{\min}), y_{\min}, y_{\max}),$$

406 where y_{\min}, y_{\max} define the interval of the rating scale, and Z represents independent Gaussian 407 noise. To verify that our findings are robust to any artifacts of this perturbation process, we 408 complement this error perturbation approach with persona ratings sampled from real LLMs. 409

4.2 SETUP DETAILS

410 **Models.** We use GPT-5 to generate synthetic “human” ratings for PRISM – i.e., used as Y in 411 our framework to obtain the ground truth target parameter θ_t . We use Claude-{\Haiku 3.5, 412 Sonnet 3.5} and GPT-{\5, 40-Mini} to generate persona ratings for DICES. We report 413 prompts, sampling temperature and decoding methods used for each LLM in Appendix E. 414

415 **Estimators.** We compare Sample Average, IPW, Persona-Based Estimation, Persona-Augmented 416 Regression (PAR), PPI++ (Angelopoulos et al., 2023b), and Recalibrated PPI (RePPI) (Ji et al., 417 2025) estimators against two doubly-robust variants: (i) *DR (Classical)*, which learns nuisance 418 functions $(\hat{\omega}, \hat{\pi})$, and (ii) *DR (Riesz)*, which uses Riesz loss minimization to directly produce an 419 estimate $\hat{\alpha}$ of α_0 . Nuisance functions were tuned via hyperparameter search (see Appendix E). 420

421 **Metrics.** We evaluate estimator quality using three metrics: *Bias (MAE)*: $|\theta_t - \hat{\theta}_t|$, absolute deviation 422 from the target parameter; *Coverage*: $\Pr(\theta_t \in [\hat{\theta}_{\text{low}}, \hat{\theta}_{\text{high}}])$, the probability that the confidence 423 interval covers the true parameter; and *Interval Width*: $\hat{\theta}_{\text{high}} - \hat{\theta}_{\text{low}}$, the length of the interval. 424

4.3 RESULTS

425 **Finding 1: DR (Riesz) obtains lower bias and improved coverage than baseline estimators.** 426 Figures 3 and 4 present our main findings varying (i) covariate shift, (ii) selection bias, and (iii) 427 persona quality over all three datasets ($N = 40$ trials per setting). We present cross-sectional 428 results in Fig. 3 and average in Fig. 4. As illustrated in Fig. 3, DR (Riesz) obtains valid 95% 429 CIs when (i) persona quality is high (top), (ii) covariate shift is moderate (middle) and (iii) across 430 ranges of selection bias (bottom). In contrast, baseline estimators obtain valid coverage only on 431 *Synthetic* when: (i) persona quality is very high (Fig. 3, top left) and (ii) and dropout rate is high

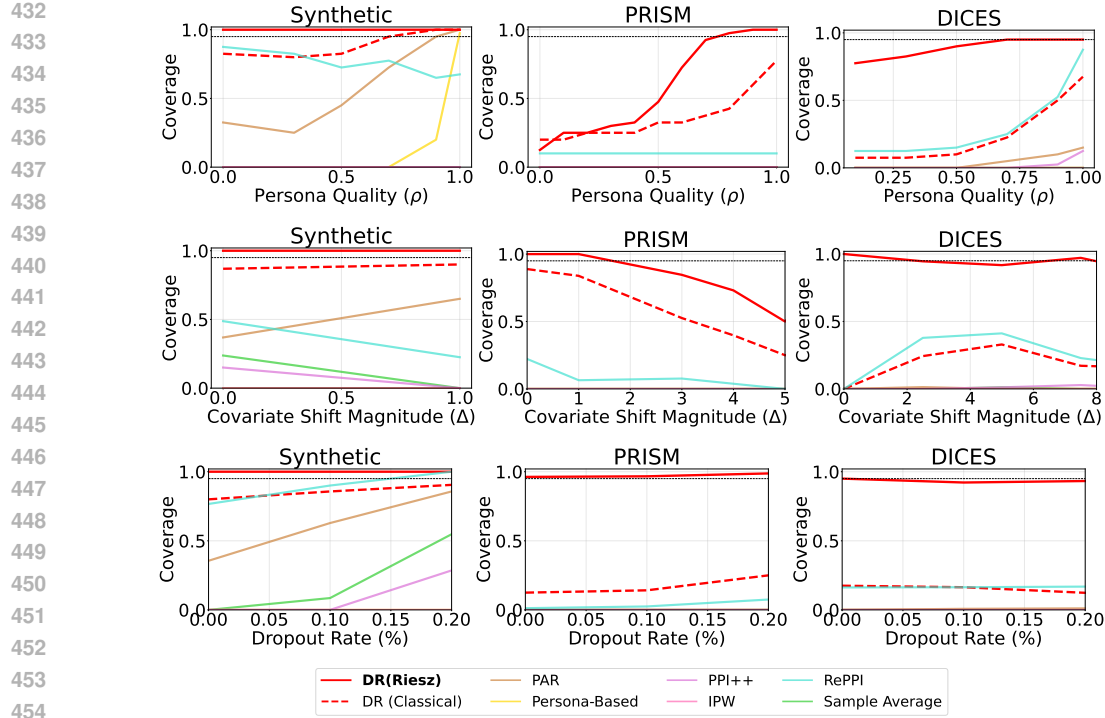


Figure 3: Coverage by persona quality (top), covariate shift (center), and selection bias (bottom). DR (Riesz) attains better coverage than all baselines. Baselines with 0% coverage omitted to reduce clutter. $\eta = 0.1$; $\rho = 0.6$ for bottom two rows. Fig. 12–14 (Appendix E) presents analogous results for Bias (MAE) and Interval Width.

Method	Synthetic			PRISM			DICES		
	Bias	Coverage	Width	Bias	Coverage	Width	Bias	Coverage	Width
Sample Average	0.73 ± 0.17	0.06 ± 0.03	0.35 ± 0.01	1.30 ± 0.02	0.00	1.49	0.10	0.00	0.07
IPW	0.48 ± 0.05	0.00	1.00 ± 0.20	25.49 ± 0.02	0.00	2.62 ± 0.03	0.17	0.07	0.10
PAR	0.06	0.44 ± 0.03	0.10	0.83 ± 0.01	0.02 ± 0.01	0.91	0.05	0.04	0.02
Persona-Based	0.37 ± 0.01	0.00	0.17	10.00 ± 0.01	0.00	1.33	0.34	0.00	0.05
PPI++	0.69 ± 0.16	0.03 ± 0.02	0.17 ± 0.01	1.03 ± 0.01	0.00	1.01	0.06	0.01	0.03
RePPI	0.10 ± 0.01	0.56 ± 0.09	0.19	0.63 ± 0.01	0.66 ± 0.02	1.36	0.04 ± 0.01	0.40	0.05
DR (Classical)	0.07	0.85 ± 0.01	0.21	0.68 ± 0.01	0.82 ± 0.02	1.75	0.05	0.32	0.06 ± 0.01
DR (Riesz)	0.03	1.00	0.28 ± 0.01	0.46 ± 0.01	0.93 ± 0.01	1.68	0.02	0.86 ± 0.01	0.09

Figure 4: Average Bias (MAE), Coverage, and Interval Width across experimental conditions presented in Fig. 3. Values in parentheses denote standard error (values < 0.01 omitted to reduce clutter).

(Fig. 3, bottom left). While counterintuitive, the second observation highlights the importance of examining covariate shift and selection bias in parallel; as dropout rate increases in *Synthetic*, the mean of remaining source samples more closely resembles that of the target distribution, leading to coincidentally higher coverage. Yet coverage remains poor on both PRISM and DICES.

Finding 2: DR (Riesz) yields improved coverage and lower bias (MAE) than DR (Classical). Across levels of covariate shift, selection bias, and persona quality, we observe DR (Riesz) (Fig. 3; solid lines) obtains improved estimates compared to DR (Classical) (Fig. 3; dashed lines). While this behavior also appears in *Synthetic* (Fig. 3; left column), the gap between DR (Classical) and DR (Riesz) is especially pronounced when learning nuisance functions on embeddings of high-dimensional text (Fig. 3; PRISM, DICES). This illustrates the importance of directly estimating the re-weighting term $\alpha_0(W, C)$ (Equation. (4)) rather than learning $\omega_0(W)$ and $\pi_0(W)$ separately.

Finding 3: DR (Riesz) makes better use of persona ratings than baseline estimators. Several of our baselines — RePPI, PAR, and Persona-Based — use persona ratings to compute estimates. However, across levels of persona quality (Fig 3; top row), DR (Riesz) produces higher quality estimates than these baselines (with valid coverage for $\rho \geq .65$ on both PRISM and DICES). Fig. 5 extends this analysis to persona ratings obtained from real LLMs on DICES. For all LLMs, we observe that

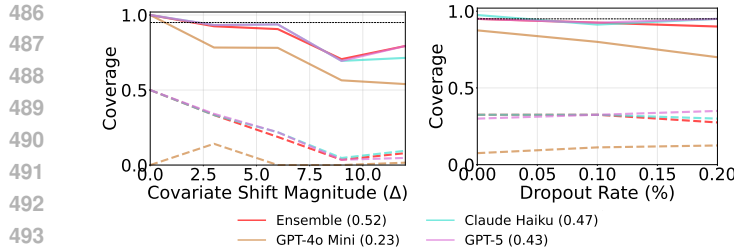


Figure 5: Coverage of DR (Riesz) (solid) versus RePPI (dashed) when varying covariate shift (left) and selection bias (right) with persona ratings from different LLM judges. Parentheses denote Pearson correlation between persona and human ratings.

coverage of DR (Riesz) (solid) is markedly higher than that of RePPI (dashed). Further substantiating our systematic perturbation study Fig. 3 (top row), we observe that real LLMs that exhibit a higher correlation with human ratings (e.g., GPT-5; $\rho = 0.43$) yield improved coverage over those with lower correlation (e.g., GPT-4o Mini; $\rho = 0.23$). Furthermore, despite having lower correlation coefficients, we observe several models achieving comparable coverage to our artificially perturbed persona ratings (Fig. 3; $\rho = 0.6$). Taken together, these findings illustrate that persona ratings from real LLMs-as-judges can be used to improve downstream estimates under evaluation sampling bias.

5 RELATED WORK

We now provide a brief overview of related literature (see Appendix A for a detailed discussion).

Automated Evaluation with Persona Prompting. To address evaluation sampling bias, one strategy is to use an automated rater to rate outputs from the target distribution. Under this LLM-as-a-judge approach, a *judge* GenAI system rates the outputs of a *target* GenAI system (Li et al., 2024; Elangovan et al., 2024; Ye et al., 2024; Bubeck et al., 2023; Zheng et al., 2023). Because human raters often disagree on criteria such as “helpfulness” or “relevance” (Kirk et al., 2024), prior work has explored instructing judge systems to adopt *personas* — descriptions of humans with specific characteristics (Castricato et al., 2024; Fröhling et al., 2024; Orlikowski et al., 2025; Deng et al., 2025). However, work has also shown that persona ratings are often an imperfect proxy for human ratings (Santurkar et al., 2023; Neumann et al., 2025). Thus, our work treats persona ratings as a *useful yet incomplete proxy* for human raters to improve GenAI system quality estimates.

Frameworks for Sample Efficient Estimation. Other works propose methods for improving statistical inference when data is scarce but ML predictions are abundant. Prediction-Powered Inference (PPI) and its computationally efficient variant PPI++ use ML predictions to tighten confidence intervals through a “rectifier term” that corrects for bias in ML predictions (Angelopoulos et al., 2023a; Chatzi et al., 2024; Fisch et al., 2024; Angelopoulos et al., 2023b). Ji et al. (2025) show PPI++ to be a special case of M-estimation with surrogate outcomes, a classical problem in causal inference (Robins et al., 1994; Robins & Rotnitzky, 1995; Tsiatis, 2006), and in turn propose recalibrated PPI (or RePPI) to offer more efficient estimation. However, these approaches fail to give valid coverage under evaluation sampling bias. We develop a doubly-robust estimator (Bang & Robins, 2005; Chernozhukov et al., 2018; 2023) that can handle covariate shift and selection bias simultaneously while making use of surrogate predictions/persona ratings. We also use “Riesz losses” (Chernozhukov et al., 2023; 2022a;b) to estimate complicated nuisance parameters using generic ML learners.

6 CONCLUSION

Our work answers calls for greater consideration of external validity concerns in Generative AI evaluation (Weidinger et al., 2025; Ibrahim et al., 2024; Liao et al., 2021; Salaudeen et al., 2025) through a theoretically rigorous and empirically validated estimation framework. Our framework provides a path forward for combining limited human ratings observed under sampling bias with imperfect persona ratings to obtain statistically valid system quality estimates. Beyond our specific doubly-robust estimation framework, our Persona Simulation Framework (PSF) also provides a reusable community resource for validating future methods designed to address sampling bias. While our framework relaxes the MCAR assumption imposed by existing estimation frameworks, it also imposes assumptions — e.g., no concept drift — on the evaluation process. Future work should also consider how violations of this and other assumptions in Appendices B and C might affect system quality estimates.

540 7 REPRODUCIBILITY STATEMENT
541

542 We take several steps to ensure the reproducibility of our work. First, we document all theoretical as-
543 sumptions required by our framework and provide complete proofs in Appendix B. Second, we pro-
544 vide thorough documentation of our experiment design, hyperparameters, and datasets required to
545 reproduce our empirical results in Appendix E. Finally, we provide code necessary to reproduce our
546 analysis in the supplementary material. We plan to release all code and datasets in our Persona Sim-
547 ulation Framework along with the paper so that the broader community can build upon our framework.
548

549 REFERENCES
550

551 Suhaib Abdurahman, Mohammad Atari, Farzan Karimi-Malekabadi, Mona J Xue, Jackson Trager,
552 Peter S Park, Preni Golazian, Ali Omrani, and Morteza Dehghani. Perils and opportunities in
553 using large language models in psychological research. *PNAS nexus*, 3(7):pgae245, 2024.

554 Anastasios N Angelopoulos, Stephen Bates, Clara Fannjiang, Michael I Jordan, and Tijana Zrnic.
555 Prediction-powered inference. *Science*, 382(6671):669–674, 2023a.

557 Anastasios N Angelopoulos, John C Duchi, and Tijana Zrnic. Ppi++: Efficient prediction-powered
558 inference. *arXiv preprint arXiv:2311.01453*, 2023b.

559 Ruicheng Ao, Hongyu Chen, and David Simchi-Levi. Prediction-guided active experiments. *arXiv*
560 *preprint arXiv:2411.12036*, 2024.

562 Lisa P Argyle, Ethan C Busby, Nancy Fulda, Joshua R Gubler, Christopher Rytting, and David
563 Wingate. Out of one, many: Using language models to simulate human samples. *Political Analysis*,
564 31(3):337–351, 2023.

566 Lora Aroyo, Alex Taylor, Mark Diaz, Christopher Homan, Alicia Parrish, Gregory Serapio-García,
567 Vinodkumar Prabhakaran, and Ding Wang. Dices dataset: Diversity in conversational ai evalua-
568 tion for safety. *Advances in Neural Information Processing Systems*, 36:53330–53342, 2023.

569 Heejung Bang and James M Robins. Doubly robust estimation in missing data and causal inference
570 models. *Biometrics*, 61(4):962–973, 2005.

572 Etienne Becht, Leland McInnes, John Healy, Charles-Antoine Dutertre, Immanuel WH Kwok,
573 Lai Guan Ng, Florent Ginhoux, and Evan W Newell. Dimensionality reduction for visualizing
574 single-cell data using umap. *Nature biotechnology*, 37(1):38–44, 2019.

575 James Bisbee, Joshua D Clinton, Cassy Dorff, Brenton Kenkel, and Jennifer M Larson. Synthetic
576 replacements for human survey data? the perils of large language models. *Political Analysis*, 32
577 (4):401–416, 2024.

579 David Broska, Michael Howes, and Austin van Loon. The mixed subjects design: Treating large
580 language models as potentially informative observations. *Sociological Methods & Research*, pp.
581 00491241251326865, 2024.

582 Sébastien Bubeck, Varun Chandrasekaran, Ronen Eldan, Johannes Gehrke, Eric Horvitz, Ece Ka-
583 mar, Peter Lee, Yin Tat Lee, Yuanzhi Li, Scott Lundberg, et al. Sparks of artificial general
584 intelligence: Early experiments with gpt-4. *arXiv preprint arXiv:2303.12712*, 2023.

586 Pengshan Cai, Fei Liu, Adarsha Bajracharya, Joe Sills, Alok Kapoor, Weisong Liu, Dan Berlowitz,
587 David Levy, Richeek Pradhan, and Hong Yu. Generation of patient after-visit summaries to
588 support physicians. In *Proceedings of the 29th International Conference on Computational Lin-*
589 *guistics (COLING)*, 2022.

590 Louis Castricato, Nathan Lile, Rafael Rafailov, Jan-Philipp Fränken, and Chelsea Finn. Persona: A
591 reproducible testbed for pluralistic alignment. *arXiv preprint arXiv:2407.17387*, 2024.

593 Ivi Chatzi, Eleni Straitouri, Suhas Thejaswi, and Manuel Gomez Rodriguez. Prediction-powered
594 ranking of large language models. *arXiv preprint arXiv:2402.17826*, 2024.

594 Victor Chernozhukov, Denis Chetverikov, Mert Demirer, Esther Duflo, Christian Hansen, Whitney
 595 Newey, and James Robins. Double/debiased machine learning for treatment and structural pa-
 596 rameters, 2018.

597

598 Victor Chernozhukov, Whitney Newey, Victor M Quintas-Martinez, and Vasilis Syrgkanis. Riesznet
 599 and forestriesz: Automatic debiased machine learning with neural nets and random forests. In
 600 *International Conference on Machine Learning*, pp. 3901–3914. PMLR, 2022a.

601 Victor Chernozhukov, Whitney K Newey, and Rahul Singh. Automatic debiased machine learning
 602 of causal and structural effects. *Econometrica*, 90(3):967–1027, 2022b.

603

604 Victor Chernozhukov, Michael Newey, Whitney K Newey, Rahul Singh, and Vasilis Srygkanis. Au-
 605 tomatic debiased machine learning for covariate shifts. *arXiv preprint arXiv:2307.04527*, 2023.

606 Wesley Hanwen Deng, Sunnie SY Kim, Akshita Jha, Ken Holstein, Motahare Eslami, Lauren
 607 Wilcox, and Leon A Gatys. Personateaming: Exploring how introducing personas can improve
 608 automated ai red-teaming. *arXiv preprint arXiv:2509.03728*, 2025.

609

610 Yijiang River Dong, Tiancheng Hu, and Nigel Collier. Can llm be a personalized judge? *arXiv
 611 preprint arXiv:2406.11657*, 2024.

612

613 Florian E Dorner, Vivian Y Nastl, and Moritz Hardt. Limits to scalable evaluation at the frontier:
 614 Llm as judge won’t beat twice the data. *arXiv preprint arXiv:2410.13341*, 2024.

615 Rick Durrett. *Probability: theory and examples*, volume 49. Cambridge university press, 2019.

616

617 Naoki Egami, Musashi Hinck, Brandon Stewart, and Hanying Wei. Using imperfect surrogates for
 618 downstream inference: Design-based supervised learning for social science applications of large
 619 language models. *Advances in Neural Information Processing Systems*, 36:68589–68601, 2023.

620

621 Naoki Egami, Musashi Hinck, Brandon M Stewart, and Hanying Wei. Using large language model
 622 annotations for the social sciences: A general framework of using predicted variables in down-
 623 stream analyses. 2024.

624

625 Aparna Elangovan, Lei Xu, Jongwoo Ko, Mahsa Elyasi, Ling Liu, Sravan Bodapati, and Dan Roth.
 626 Beyond correlation: The impact of human uncertainty in measuring the effectiveness of automatic
 627 evaluation and llm-as-a-judge. *arXiv preprint arXiv:2410.03775*, 2024.

628

629 Benjamin Eyre and David Madras. Auto-evaluation with few labels through post-hoc regression.
 630 *arXiv preprint arXiv:2411.12665*, 2024.

631

632 Jean Feydy, Thibault Séjourné, François-Xavier Vialard, Shun-ichi Amari, Alain Trouve, and
 633 Gabriel Peyré. Interpolating between optimal transport and mmd using sinkhorn divergences.
 634 In *The 22nd International Conference on Artificial Intelligence and Statistics*, pp. 2681–2690,
 635 2019.

636

637 Michael G Findley, Kyosuke Kikuta, and Michael Denly. External validity. *Annual review of politi-
 638 cal science*, 24(1):365–393, 2021.

639

640 Adam Fisch, Joshua Maynez, R Alex Hofer, Bhuwan Dhingra, Amir Globerson, and William W
 641 Cohen. Stratified prediction-powered inference for hybrid language model evaluation. *arXiv
 642 preprint arXiv:2406.04291*, 2024.

643

644 Riccardo Fogliato, Pratik Patil, Mathew Monfort, and Pietro Perona. A framework for efficient
 645 model evaluation through stratification, sampling, and estimation. In *European Conference on
 646 Computer Vision*, pp. 140–158. Springer, 2024.

647

648 Leon Fröhling, Gianluca Demartini, and Dennis Assenmacher. Personas with attitudes: Controlling
 649 llms for diverse data annotation. *arXiv preprint arXiv:2410.11745*, 2024.

650

651 Joseph K Goodman and Gabriele Paolacci. Crowdsourcing consumer research. *Journal of Consumer
 652 Research*, 44(1):196–210, 2017.

648 Gloria Guzman and Melissa Kollar. Income in the united states: 2022. *United States Census*
 649 *Bureau. https://www.census.gov/content/dam/Census/library/publications/2023/demo/p60-279.*
 650 *pdf*, 2023.

651

652 David A Hirshberg and Stefan Wager. Augmented minimax linear estimation. *The Annals of Statistics*, 49(6):3206–3227, 2021.

653

654 Pei-Yun Hsueh, Prem Melville, and Vikas Sindhwani. Data quality from crowdsourcing: a study
 655 of annotation selection criteria. In *Proceedings of the NAACL HLT 2009 workshop on active*
 656 *learning for natural language processing*, pp. 27–35, 2009.

657

658 Lujain Ibrahim, Saffron Huang, Lama Ahmad, and Markus Anderljung. Beyond static ai eval-
 659 uations: advancing human interaction evaluations for llm harms and risks. *arXiv preprint*
 660 *arXiv:2405.10632*, 2024.

661

662 Wenlong Ji, Lihua Lei, and Tijana Zrnic. Predictions as surrogates: Revisiting surrogate outcomes
 663 in the age of ai. *arXiv preprint arXiv:2501.09731*, 2025.

664

665 Hannah Rose Kirk, Alexander Whitefield, Paul Rottger, Andrew M Bean, Katerina Margatina,
 666 Rafael Mosquera-Gomez, Juan Ciro, Max Bartolo, Adina Williams, He He, et al. The prism
 667 alignment dataset: What participatory, representative and individualised human feedback reveals
 668 about the subjective and multicultural alignment of large language models. *Advances in Neural*
Information Processing Systems, 37:105236–105344, 2024.

669

670 Tobias Leemann, Periklis Petridis, Giuseppe Vietri, Dionysis Manousakas, Aaron Roth, and Sergul
 671 Aydore. Auto-gda: Automatic domain adaptation for efficient grounding verification in retrieval
 672 augmented generation. *arXiv preprint arXiv:2410.03461*, 2024.

673

674 Kevin E Levay, Jeremy Freese, and James N Druckman. The demographic and political composition
 675 of mechanical turk samples. *Sage Open*, 6(1):2158244016636433, 2016.

676

677 Dawei Li, Bohan Jiang, Liangjie Huang, Alimohammad Beigi, Chengshuai Zhao, Zhen Tan, Amrita
 678 Bhattacharjee, Yuxuan Jiang, Canyu Chen, Tianhao Wu, et al. From generation to judgment:
 Opportunities and challenges of llm-as-a-judge. *arXiv preprint arXiv:2411.16594*, 2024.

679

680 Q Vera Liao and Ziang Xiao. Rethinking model evaluation as narrowing the socio-technical gap.
 681 *arXiv preprint arXiv:2306.03100*, 2023.

682

683 Thomas Liao, Rohan Taori, Inioluwa Deborah Raji, and Ludwig Schmidt. Are we learning yet? a
 684 meta review of evaluation failures across machine learning. In *Thirty-fifth Conference on Neural*
Information Processing Systems Datasets and Benchmarks Track (Round 2), 2021.

685

686 Kevin J Mullinix, Thomas J Leeper, James N Druckman, and Jeremy Freese. The generalizability
 687 of survey experiments. *Journal of Experimental Political Science*, 2(2):109–138, 2015.

688

689 Terrence Neumann, Maria De-Arteaga, and Sina Fazelpour. Should you use llms to simulate opin-
 690 ions? quality checks for early-stage deliberation, 2025. URL <https://arxiv.org/abs/2504.08954>.

691

692 Whitney K Newey and Daniel McFadden. Large sample estimation and hypothesis testing. *Hand-
 693 book of econometrics*, 4:2111–2245, 1994.

694

695 Jerzy Neyman. C (α) tests and their use. *Sankhyā: The Indian Journal of Statistics, Series A*, pp.
 1–21, 1979.

696

697 Matthias Orlikowski, Jiaxin Pei, Paul Röttger, Philipp Cimiano, David Jurgens, and Dirk Hovy.
 698 Beyond demographics: Fine-tuning large language models to predict individuals’ subjective text
 699 perceptions. *arXiv preprint arXiv:2502.20897*, 2025.

700

701 Siru Ouyang, Shuohang Wang, Yang Liu, Ming Zhong, Yizhu Jiao, Dan Iter, Reid Pryzant, Chen-
 guang Zhu, Heng Ji, and Jiawei Han. The shifted and the overlooked: A task-oriented investiga-
 702 tion of user-gpt interactions. *arXiv preprint arXiv:2310.12418*, 2023.

702 Peter S Park, Philipp Schoenegger, and Chongyang Zhu. Diminished diversity-of-thought in a stan-
 703 dard large language model. *Behavior Research Methods*, 56(6):5754–5770, 2024.
 704

705 Yijiang River Dong, Tiancheng Hu, Yinhong Liu, Ahmet Üstün, and Nigel Collier. When personal-
 706 ization meets reality: A multi-faceted analysis of personalized preference learning. *arXiv e-prints*,
 707 pp. arXiv–2502, 2025.

708 James M Robins and Andrea Rotnitzky. Semiparametric efficiency in multivariate regression models
 709 with missing data. *Journal of the American Statistical Association*, 90(429):122–129, 1995.
 710

711 James M Robins, Andrea Rotnitzky, and Lue Ping Zhao. Estimation of regression coefficients when
 712 some regressors are not always observed. *Journal of the American statistical Association*, 89
 713 (427):846–866, 1994.

714 Jon Saad-Falcon, Omar Khattab, Christopher Potts, and Matei Zaharia. Ares: An automated eval-
 715 uation framework for retrieval-augmented generation systems. *arXiv preprint arXiv:2311.09476*,
 716 2023.

717 Olawale Salaudeen, Anka Reuel, Ahmed Ahmed, Suhana Bedi, Zachary Robertson, Sudharsan Sun-
 718 dar, Ben Domingue, Angelina Wang, and Sanmi Koyejo. Measurement to meaning: A validity-
 719 centered framework for ai evaluation. *arXiv preprint arXiv:2505.10573*, 2025.

720

721 Shibani Santurkar, Esin Durmus, Faisal Ladhak, Cino Lee, Percy Liang, and Tatsunori Hashimoto.
 722 Whose opinions do language models reflect? In *International Conference on Machine Learning*,
 723 pp. 29971–30004. PMLR, 2023.

724 Kazuhiro Takemoto. The moral machine experiment on large language models. *Royal Society open
 725 science*, 11(2):231393, 2024.

726

727 Anastasios A Tsiatis. *Semiparametric theory and missing data*, volume 4. Springer, 2006.

728

729 Aad W Van der Vaart. *Asymptotic statistics*, volume 3. Cambridge university press, 2000.

730

731 Laura Weidinger, Inioluwa Deborah Raji, Hanna Wallach, Margaret Mitchell, Angelina Wang,
 732 Olawale Salaudeen, Rishi Bommasani, Deep Ganguli, Sanmi Koyejo, and William Isaac. To-
 733 toward an evaluation science for generative ai systems. *arXiv preprint arXiv:2503.05336*, 2025.

734

735 Dustin Wright, Arnav Arora, Nadav Borenstein, Srishti Yadav, Serge Belongie, and Isabelle Augen-
 736 stein. LLM tropes: Revealing fine-grained values and opinions in large language models. In Yaser
 737 Al-Onaizan, Mohit Bansal, and Yun-Nung Chen (eds.), *Findings of the Association for Compu-
 738 tational Linguistics: EMNLP 2024*, pp. 17085–17112, Miami, Florida, USA, November 2024.
 739 Association for Computational Linguistics. doi: 10.18653/v1/2024.findings-emnlp.995. URL
 740 <https://aclanthology.org/2024.findings-emnlp.995/>.

741

742 Zichun Xu, Daniela Witten, and Ali Shojaie. A unified framework for semiparametrically efficient
 743 semi-supervised learning. *arXiv preprint arXiv:2502.17741*, 2025.

744

745 Jiayi Ye, Yanbo Wang, Yue Huang, Dongping Chen, Qihui Zhang, Nuno Moniz, Tian Gao, Werner
 746 Geyer, Chao Huang, Pin-Yu Chen, et al. Justice or prejudice? quantifying biases in llm-as-a-
 747 judge. *arXiv preprint arXiv:2410.02736*, 2024.

748

749 Lianmin Zheng, Wei-Lin Chiang, Ying Sheng, Siyuan Zhuang, Zhanghao Wu, Yonghao Zhuang,
 750 Zi Lin, Zhuohan Li, Dacheng Li, Eric Xing, et al. Judging llm-as-a-judge with mt-bench and
 751 chatbot arena. *Advances in Neural Information Processing Systems*, 36:46595–46623, 2023.

752

753 Haotian Zhou and Ayelet Fishbach. The pitfall of experimenting on the web: How unattended
 754 selective attrition leads to surprising (yet false) research conclusions. *Journal of personality and
 755 social psychology*, 111(4):493, 2016.

756
757

This Appendix is organized as follows:

758

- Appendix A provides an extended discussion of related work.
- Appendix B provides formal setup of our framework, notation, and theoretical results.
- We extend our analysis to general M-estimators under covariate shift with surrogate (persona) ratings in Appendix C. We provide a general proof, from which our results in Appendix B follow.
- Appendix D provides details on our Riesz loss minimizer used to perform re-weighting.
- Appendix E details our experimental setup and provides additional empirical results.

760

761

762

763

764

765

766

767

768

769

770

771

772

773

A EXTENDED RELATED WORK

774

775

A.1 THREATS TO THE EXTERNAL VALIDITY OF GENERATIVE AI EVALUATIONS

776

777

778

779

780

781

782

783

784

In the quantitative social sciences, external validity describes the extent to which findings from a study generalize to different populations, settings, and times (Findley et al., 2021). Threats to external validity have long been studied in survey research. For example, Levay et al. (2016) found notable discrepancies between the demographic composition of convenience samples obtained via Amazon Mechanical Turk (MTurk) versus nationally representative American National Election Study (ANES) samples. While Mullinix et al. (2015) observe that study findings often remain robust to such discrepancies, (Zhou & Fishbach, 2016) demonstrate that *differential non-compliance* — a form of selection bias in which participants drop out from studies non-randomly — can have substantive effects on studies’ results. Myriad factors contribute to this selection bias, such as participants’ motivation and language skills (Goodman & Paolacci, 2017).

785

786

787

788

789

790

791

792

793

794

795

796

797

798

799

More recently, concerns have emerged surrounding the *external validity* of evaluations obtained from general purpose benchmarks (e.g., MMLU, BigBench) and leaderboards (e.g., Chatbot Arena) (Ibrahim et al., 2024; Ouyang et al., 2023; Liao & Xiao, 2023). As with survey research, GenAI performance measurements can be subject to covariate shift when the distribution of system outputs or human raters differs between a lab-based evaluation and target deployment context (Saad-Falcon et al., 2023; Leemann et al., 2024; Kirk et al., 2024). Likewise, *differential non-compliance* can occur when raters in online rating platforms drop-out due to failed quality checks (e.g., due to poor English language proficiency) (Hsueh et al., 2009). Such selection bias can confound results if common factors (e.g., English language proficiency) affect rater drop-out and their ratings. Selection bias can also arise if some raters are more likely to voluntarily assign ratings than others — e.g., when busy physicians rate complex system outputs less frequently than more available medical students. While growing work has highlighted external validity as an important desideratum for evaluations (Ibrahim et al., 2024; Ouyang et al., 2023; Liao & Xiao, 2023), to our knowledge, no existing statistical frameworks simultaneously address covariate shift, selection bias, and high-dimensional model outputs while leveraging imperfect automated ratings.

800

801

802

803

804

805

806

807

808

809

We address this gap by developing a statistical framework for characterizing and mitigating threats to the external validity of GenAI performance evaluations. We devise a data-efficient estimator that corrects for covariate shift and selection bias in parallel, given ratings from a source population and predictions generated by a black-box machine learning model over both source and target populations. Some advances in our framework provide a new perspective on classic methodological challenges in survey research. For example, we provide a doubly-robust alternative to the reweighting estimators traditionally used to correct for selection bias. This approach obtains valid coverage even when the re-weighting model is misspecified. Our framework also addresses novel challenges that arise in the GenAI evaluation context. In particular, we leverage embeddings to support robust statistical inference over high-dimensional model output spaces (e.g., text, image) as opposed to the structured data formats traditionally used for survey research. Central to our approach is the principled adoption of *synthetic ratings* generated by an AI persona, which we discuss next.

810 A.2 AUTOMATED EVALUATION WITH LLM-AS-A-JUDGE AND PERSONA PROMPTING
811

812 Given the cost and scalability challenges associated with collecting human ratings, automated meth-
813 ods are increasingly used to scale up evaluation workflows traditionally performed by humans. In
814 particular, the LLM-as-a-judge paradigm introduces a second *judge* GenAI system to evaluate the
815 outputs returned by a *target* GenAI system (Li et al., 2024; Elangovan et al., 2024; Ye et al., 2024;
816 Bubeck et al., 2023; Zheng et al., 2023). Because human raters can disagree as to whether a model
817 output is “helpful”, or “relevant” (Kirk et al., 2024), recent work has proposed instructing judge sys-
818 tems to adopt personas—that is, descriptions of humans with specific sociodemographic characteris-
819 tics, such as gender and race (Castricato et al., 2024; Dong et al., 2024; Fröhling et al., 2024; Wright
820 et al., 2024; Orlikowski et al., 2025; River Dong et al., 2025). This persona-based prompting strategy
821 is designed to better-account for sources of rater-specific variation throughout the evaluation process.
822

823 These automated evaluation methods offer a promising approach to mitigate the external validity
824 threats described in § A.1. In particular, judge systems with persona prompting can generate
825 low-cost synthetic ratings when human ratings from the target population are limited. However,
826 because such ratings may be systematically biased (Santurkar et al., 2023; Neumann et al., 2025),
827 their direct adoption in evaluation pipelines may yield biased performance measurements. Our
828 proposed doubly-robust approach addresses this challenge by treating LLM-as-a-judge ratings as
829 *potentially informative yet biased proxies* for human ratings. This approach combines surrogate
830 ratings with human ratings (observed under evaluation sampling bias) to obtain statistically valid
831 confidence intervals in the target population of interest.

832 A.3 GENAI SYSTEMS AS HUMAN SURROGATES IN SOCIAL SCIENCE STUDIES
833

834 While our work foregrounds GenAI evaluation challenges, it bears conceptual and methodological
835 similarity to work investigating GenAI systems as surrogates for human subjects in social science
836 studies. Inline with the turn towards crowdworkers as a low-cost surrogate for target study popu-
837 lations (§ A.1), this growing line of work introduces GenAI systems as a surrogate for more costly
838 human subjects (Argyle et al., 2023). Notably, such work often targets the very same statistical
839 parameters recovered by our general M-estimation framework (Table 1). For example, let v denote
840 an item in an opinion poll (e.g., “*do you believe in the right to bear arms?*”), let X denote rater
841 characteristics (e.g., locale and demographics, per (Santurkar et al., 2023)), and let Y represent a
842 binary response (endorse/not endorse) to the survey item. The parameter

$$\theta_t(v) := \mathbb{E}_t[Y \mid V = v] \quad (5)$$

843 denotes the proportion of raters in the target population who endorse this survey item. Thus, re-
844 searchers can also leverage our methodology when using GenAI systems as surrogates for human
845 subjects in social science studies. Given a finite sample of human ratings from the source popu-
846 lation $\{(X_i, V_i, Y_i)\}_{i=1}^N \sim P_s$, and surrogate data produced for the source and target population,
847 researchers can recover informative and statistically valid confidence intervals for parameters de-
848 fined over the target population of human subjects.

849 Given the overlap between our motivating application and social science studies, we also discuss
850 methods advancing the principled adoption of GenAI systems as surrogate data in social science
851 research (Broska et al., 2024; Egami et al., 2024; 2023). These works view surrogate data as a
852 flawed (Bisbee et al., 2024; Park et al., 2024; Takemoto, 2024; Abdurahman et al., 2024) but po-
853 tentially informative source of information for statistical inference in social science studies. For
854 instance, Broska et al. (2024) leverage prediction powered inference (Angelopoulos et al., 2023a)
855 to correct for bias in surrogate data. However, as discussed in § A.4, PPI is vulnerable to covari-
856 ate shift and selection bias between source and target study populations. Most related to our work,
857 (Egami et al., 2024; 2023) introduce a doubly robust estimation approach that generalizes PPI by
858 applying a bias-correction to the underlying moment function (as opposed to the outcome variable).
859 Critically, however, this approach takes a design-based sampling procedure, which assumes that the
860 probability of labeling a sample is known by the researcher in advance. This precludes the more
861 general setting we study in our work, in which the reweighting function is unknown in advance.⁵

862
863 ⁵As noted in (Egami et al., 2024; 2023), this design-based sampling approach is well-motivated when the
864 full corpus of documents to be annotated and corresponding sampling probabilities are known in advance.

864 Having discussed both GenAI and social science applications of our framework, we now turn to the
 865 underlying statistical methodology we advance in this work.
 866

867 **A.4 STATISTICAL FRAMEWORKS FOR SAMPLE EFFICIENT-ESTIMATION**
 868

869 Recent developments in black-box predictive models that can operate on multi-modal representations
 870 has spurred significant interest in how these predictions might be used to improve statistical
 871 inference (Angelopoulos et al., 2023a;b; Fisch et al., 2024; Eyre & Madras, 2024; Dorner et al.,
 872 2024; Ji et al., 2025; Saad-Falcon et al., 2023; Fogliato et al., 2024). These frameworks address the
 873 challenge of making valid statistical inferences when labeled data is scarce but black-box predictions
 874 cheap and abundant. We briefly review developments in this literature before identifying key
 875 gaps addressed by our approach.
 876

877 Prediction-Powered Inference (PPI) uses predictions from a black-box machine learning model to
 878 tighten confidence intervals when labeled data is scarce (Angelopoulos et al., 2023a;b). This is
 879 done through the addition of a “rectifier” — a mean zero term that contrasts the performance of
 880 the model’s predictions on the labeled and unlabeled points. While initial variants of PPI were not
 881 computationally efficient, Angelopoulos et al. (2023b) introduce a PPI++ framework, which intro-
 882 duces a “trust” parameter λ to control the magnitude of the rectifier. This allows for efficiently
 883 computable confidence sets that are provably tighter than those computed just from labeled data.
 884 We also emphasize recent work due to Ji et al. (2025), which shows that PPI++ is just a special
 885 parametric class of solutions for M-estimation with surrogates outcomes — a classical, well-studied
 886 problem in the causal inference/missing data literature (Robins et al., 1994; Robins & Rotnitzky,
 887 1995; Tsiatis, 2006). While the authors do not directly mention Neyman orthogonal scores (Ney-
 888 man, 1979; Chernozhukov et al., 2018) in their work, they construct what is implicitly a Neyman
 889 orthogonal score for the problem at hand and propose a solution based on cross-fitting. Additional
 890 theoretical developments along these lines have been proposed — Ao et al. (2024) propose a frame-
 891 work for adaptive estimation of linear functionals based on supplied predictions. Likewise, Xu et al.
 892 (2025) consider a general semi-parametric framework for estimating functionals of the data gener-
 893 ating distribution in the presence of ML predictions. However, none of the aforementioned works
 894 provides a framework usable in settings where (a) unlabeled and labeled samples come from differ-
 895 ent distributions (i.e. covariate shift) and (b) data is missing at random (MAR), (i.e. the probability
 896 that outcomes are observed for any given individual depend on their features). We close this gap
 897 by proposing a doubly-robust estimator (Bang & Robins, 2005) and a general algorithm based on
 898 cross-fitting (Chernozhukov et al., 2018) for solving M-estimation problems in the presence of both
 899 covariate shift and heterogeneity in data missingness. We also incorporate recent ideas on “Riesz
 900 losses” (Chernozhukov et al., 2022b; 2023; 2022a; Hirshberg & Wager, 2021), loss functions that
 901 specify complicated nuisance functions as their minimizers. By using Riesz losses to learn the re-
 902 weighting function $\alpha_0(W, C)$, we avoid constructing plug-in estimates for ω_0 and π_0 and computing
 903 their quotient, which can result in high bias.
 904
 905
 906
 907
 908
 909
 910
 911
 912
 913
 914
 915

916 However, this assumption is violated in our setting, in which the true source/target distribution weights are
 917 unknown. As a result, the framework proposed by (Egami et al., 2024; 2023) is not directly applicable in our
 918 motivating setting with evaluation sampling bias.

918 B ASSUMPTIONS, NOTATION, AND RESULTS FROM SECTION 3

919 920 B.1 ASSUMPTIONS ON DATA-GENERATING DISTRIBUTIONS

921
922 We start by formally describing the data generating processes considered throughout the paper. We
923 start by describing the assumptions we place of the “full-data” source and target distributions.

924 **Assumption 1.** We assume there are two “full data” distributions over tuples (X, V, C, \hat{Y}, Y) : a
925 *source distribution* P_s and a *target distribution* P_t . For simplicity, we let $W = (X, V)$ denote the
926 extended set of covariates, and assume $W \in \mathcal{W}$ where \mathcal{W} is some generic measurable space. We
927 assume the following hold:

928 1. (*No Concept Drift*) The conditional distribution of Y given W is the same under P_s and
929 P_t , i.e. for any w

$$930 \quad P_s(Y \in E \mid W = w) = P_t(Y \in E \mid W = w)$$

931 for any event E .

932 2. (*Surrogates are Functions of the Data*) The observed surrogate \hat{Y} satisfies:

$$933 \quad \hat{Y} = f(X, V, \epsilon),$$

934 where ϵ is a random variable independent of the vector (X, V, C, Y) .

935 3. (*Positivity*) We have

$$936 \quad 0 < \pi_0(W) \leq 1 \quad \text{where} \quad \pi_0(w) := P_s(C = 1 \mid W = w).$$

937 4. (*Conditional Ignorability Under Source*) The outcome Y is conditionally independent of
938 C given extended covariates W , i.e. we have

$$939 \quad Y \perp\!\!\!\perp C \mid W,$$

940 where the conditional independence is under P_s .

941 5. (*Overlap*) The likelihood/density ratio of W between P_t and P_s , defined as

$$942 \quad \omega_0(w) := \frac{dP_t}{dP_s}(w)$$

943 exists and is finite almost surely.

944 We may interchangeably write P^b or P_b for $b \in \{s, t\}$ as the distribution over source and target
945 samples, and \mathbb{E}^b and \mathbb{E}_b interchangeably as the corresponding expectations. We typically write
946 $(X^b, V^b, C^b, Y^b, \hat{Y}^b)$ and $W^b = (X^b, V^b)$ for samples drawn from P_b .

947 We briefly parse the above assumptions. The first simply says that even if the distribution of
948 $W = (X, V)$ changes wildly, the conditional distribution of Y remains the same. The second
949 assumption regards the predictions/surrogate outcomes and is trivially satisfied if \hat{Y} is the prediction
950 of a generative AI model that depends only on W and independent, external sources of randomness.
951 The third assumption, positivity, states that under the source distribution there is always some proba-
952 bility we observe the true outcome. The fourth assumption is an analogue to conditional ignorability
953 from the causal inference literature, and says that the outcome Y is conditionally independent of
954 whether or not data is observed given covariates. We note that, under the above assumptions, \hat{Y} is
955 also conditionally independent of Y and C given W . Lastly, the final assumption guarantees *overlap*,
956 or that the support of P_t is contained in the support of P_s — a necessary assumption in order to
957 perform inference under covariate shift.

958 The above assumption concerns fully-observed data — in practice, the learner will only ever observe
959 outcomes for samples where $C = 1$. That is, there is partial-observation of outcomes in the source
960 population, but outcomes are entirely absent in the target population. We formalize this in the
961 following assumption.

962 **Assumption 2.** The learner only ever observes Y for samples where $C = 1$. In other words,
963 observed samples from each distribution take the following form:

972 1. (*Source Samples*) The learner observes samples of the form $Z^s = (X^s, V^s, C^s, C^s \cdot$
 973 $Y^s, \hat{Y}^s)$ from P_s .
 974

975 2. (*Target Samples*) The learner observes samples of the form $Z^t = (X^t, V^t, \hat{Y}^t)$ from P_t .
 976

977 An important consequence of Assumption 1 is that, even when only observe partial data (per Ass-
 978 sumption 2), we can still identify general classes of estimands under the target distribution P_t . This
 979 is clarified in the following lemma.

980 **Lemma B.1.** *Let f be an arbitrary function of (Y, \hat{Y}, W) . Then, we have*

$$982 \mathbb{E}_t[f(Y^t, \hat{Y}^t, W^t)] = \mathbb{E}_s[\alpha_0(W^s, C^s)f(Y^s, \hat{Y}^s, W^s)],$$

$$983 \text{where } \alpha_0(w, c) := c \frac{\omega_0(w)}{\pi_0(w)}.$$

985 *Proof.* Observe that we have:

$$\begin{aligned} 987 \mathbb{E}_s[\alpha_0(W^s, C^s)f(Y^s, \hat{Y}^s, W^s)] &= \mathbb{E}_s\left[C^s \frac{\omega_0(W^s)}{\pi_0(W^s)} f(Y^s, \hat{Y}^s, W^s)\right] \\ 988 &= \mathbb{E}_s\left[\frac{\omega_0(W^s)}{\pi_0(W^s)} \mathbb{E}\left(C^s f(Y^s, \hat{Y}^s, W^s) \mid W^s\right)\right] \\ 989 &= \mathbb{E}_s\left[\frac{\omega_0(W^s)}{\pi_0(W^s)} \mathbb{E}(C^s \mid W^s) \mathbb{E}\left(f(Y^s, \hat{Y}^s, W^s) \mid W^s\right)\right] \\ 990 &= \mathbb{E}_s\left[\omega_0(W^s) \mathbb{E}\left(f(Y^s, \hat{Y}^s, W^s) \mid W^s\right)\right] \\ 991 &= \mathbb{E}_s\left[\omega_0(W^s) f(Y^s, \hat{Y}^s, W^s)\right] \\ 992 &= \mathbb{E}_s[f(Y^s, \hat{Y}^s, W^s)] \\ 993 &= \mathbb{E}_t[f(Y^t, \hat{Y}^t, W^t)]. \\ 994 \end{aligned}$$

995 In the above, the second equality follows from the tower rule for conditional expectations. The third
 996 follows from conditional independence, i.e. that $C^s \perp\!\!\!\perp Y^s, \hat{Y}^s \mid W^s$. The fourth equality follows by
 997 definition of $\pi_0(W^s)$. The last equality follows since $\omega_0(W^s) = \frac{dP_t}{dP_s}(W^s)$ and since the conditional
 998 distribution of (Y, \hat{Y}) is the same under P_t and P_s .
 999

□

1006 B.2 NOTATION

1008 We now discuss some additional notation that will be leveraged in the sequel.

1009 We will need to condition on independent, random nuisance estimates regularly in the sequel. For
 1010 $b \in \{s, t\}$, if U is another random variable (e.g. $U = \hat{g}$ where \hat{g} denotes a generic nuisance estimate)
 1011 and $f(Z, U)$ is some generic function, we define P_Z^b and \mathbb{E}_Z^b as the distribution and expectation over
 1012 just the randomness in Z while conditioning on U , i.e.

$$1013 P_Z^b(f(Z, U) \in E) := P_b(f(Z, U) \in E \mid U) \quad \text{and} \quad \mathbb{E}_Z^b f(Z, U) := \mathbb{E}_Z^b(f(Z, U) \mid U).$$

1015 We define the empirical distributions with respect to observations as $\mathbb{P}_{N_s} := \frac{1}{N_s} \sum_{j=1}^{N_s} \delta_{Z_i^s}$ and
 1016 $\mathbb{P}_{N_t} := \frac{1}{N_t} \sum_{i=1}^{N_t} \delta_{Z_i^t}$, where δ_z denotes the point-mass distribution on z . Thus, for a general random
 1017 function \hat{g} of data Z^b , we have $\mathbb{P}_{N_s} \hat{g}(Z^s) := \frac{1}{N_s} \sum_{j=1}^{N_s} \hat{g}(Z_j^s)$ and $\mathbb{P}_{N_t} \hat{g}(Z^t) := \frac{1}{N_t} \sum_{i=1}^{N_t} \hat{g}(Z_i^t)$.
 1018 We define the $L^2(P_Z^b)$ norm of a potentially random \mathbb{R}^d -valued function \hat{g} depending on a subset of
 1019 features $S \subset Z$ as

$$1022 \|\hat{g}\|_{L^2(P_Z^b)} := (\mathbb{E}_Z^b [\|\hat{g}(S)\|_2^2])^{1/2} = (\mathbb{E}_b (\|\hat{g}(S)\|_2^2 \mid \hat{g}))^{1/2}.$$

1023 We likewise define the $L^\infty(P_Z^b)$ norm \hat{g} as the $\|\hat{g}\|_{L^\infty(P_Z^b)} := \inf \{b \in \mathbb{R} : P_Z^b(\|\hat{g}\|_\infty > b) = 0\}$,
 1024 where $\|x\|_\infty := \max\{x_1, \dots, x_d\}$. Note that whenever \hat{g} is random, these norms are random
 1025 variables as well.

Given a (random or deterministic) sequence $(X_n)_{n \geq 1}$ in a normed space $(\mathcal{X}, \|\cdot\|)$ and a deterministic scalar sequence $(b_n)_{n \geq 1}$, we say $X_n = o(b_n)$ if $\lim_{n \rightarrow \infty} \frac{\|X_n\|}{b_n} = 0$ almost surely and $X_n = O(b_n)$ if there exists a constant $B > 0$ such that $\frac{\|X_n\|}{b_n} \leq B$ for all $n \geq 1$. We say a sequence of random variables $(X_n)_{n \geq 1}$ converges in probability to zero, denoted by $X_n \xrightarrow[n \rightarrow \infty]{\mathbb{P}} 0$, if we have

$$\lim_{n \rightarrow \infty} \mathbb{P}(\|X_n\| \geq \epsilon) = 0 \quad \text{for any } \epsilon > 0.$$

We say $X_n = o_{\mathbb{P}}(b_n)$ if $X_n/b_n \xrightarrow{\mathbb{P}} 0$, and $X_n = O_{\mathbb{P}}(b_n)$ if for any $\epsilon > 0$, there is a constant $M_\epsilon > 0$ such that $\limsup_{n \rightarrow \infty} \mathbb{P}(\|X_n\|/b_n \geq M_\epsilon) \leq \epsilon$.

If $(X_n)_{n \geq 0}$ is a sequence of random variables in \mathbb{R}^d , we always refer convergence in probability with respect to the ℓ_2 -norm, where $\|x\|_p := \left(\sum_{k=1}^d x_k^p\right)^{1/p}$ for any $1 \leq p < \infty$. Likewise, if $(X_n)_{n \geq 0}$ is a sequence of random matrices, we assume convergence in probability is defined with respect to the operator norm $\|X\|_{op} := \sup_{\substack{u \in \mathbb{R}^d \\ \|u\|_2=1}} \|Xu\|_2$. For a non-singular matrix $A \in \mathbb{R}^{d \times d}$,

we let A^{-1} denote its inverse, and A^{-T} denote the transpose of the inverse. If $x \in \mathbb{R}^d$ is a vector, we let $x^{\otimes 2} := xx^\top$ for convenience.

B.3 GENERAL DE-BIASED INFERENCE FOR AN EXPECTED OUTCOME

We now state and prove our main theorem for performing inference on an expected outcome $\theta_t = \mathbb{E}_t[Y^t]$ under evaluation sampling bias (i.e. covariate shift and selection bias). We start by stating a result that assumes the learner is given nuisance estimates that are independent of the entire sample of data. In the sequel, we describe an extended, cross-fitting based result that makes more efficient use of the data.

Theorem B.2. *Suppose Assumption 1 holds, and assume the learner has access to mutually independent samples $Z_1^s, \dots, Z_{N_s}^s$ from P_s and $Z_1^t, \dots, Z_{N_t}^t$ from P_t , as outlined in Assumption 2. Let $\mu_0(w)$ and $\alpha_0(w, s)$ be true, unknown nuisances given by*

$$\mu_0(w) := \mathbb{E}_t[Y^t \mid W^t = w] = \mathbb{E}_s[Y^s \mid W^s = w] \quad \text{and} \quad \alpha_0(w, c) = \frac{c\omega_0(w)}{\pi_0(w)},$$

where $\pi_0(w) := P_s(C^s = 1 \mid W^s = w)$ and $\omega_0(w) = \frac{dP_t}{dP_s}(w)$. Assume the following conditions hold.

1. (Ratio of Sample Sizes) There is some constant $0 < \gamma < \infty$ such that $N_t/N_s \rightarrow \gamma$.

2. (Nuisance Convergence) We have access to estimates $\hat{\mu}, \hat{\alpha}$ that are independent of the sample such that

$$\|\hat{\mu} - \mu_0\|_{L^2(P_Z^b)}, \|\hat{\alpha} - \alpha_0\|_{L^2(P_Z^b)} = o_{\mathbb{P}}(1)$$

and

$$\|\hat{\mu} - \mu_0\|_{L^2(P_Z^b)} \cdot \|\hat{\alpha} - \alpha_0\|_{L^2(P_Z^b)} = o_{\mathbb{P}}(N_t^{-1/2})$$

for $b \in \{s, t\}$. Further, we assume $\hat{\alpha}(w, 0) = 0$.

3. (Boundedness) The representer $\alpha_0(W^s, C^s)$ and the outcomes Y^s are almost surely bounded.

Let the estimator $\hat{\theta}$ be defined via the de-biased equation

$$\hat{\theta} := \mathbb{P}_{N_t} \hat{\mu}(W^t, \hat{Y}^t) + \mathbb{P}_{N_s} \hat{\alpha}(W^s, C^s) \left\{ Y^s - \hat{\mu}(W^s, \hat{Y}^s) \right\}.$$

Then, we have asymptotic linearity, i.e.

$$\sqrt{N_t}(\hat{\theta} - \theta_t) = \frac{1}{\sqrt{N_t}} \sum_{i=1}^{N_t} \mu_0(W_i^t) + \frac{\gamma}{\sqrt{N_t}} \sum_{j=1}^{N_s} \alpha_0(W_j^s, C_j^s) \{Y_j^s - \mu_0(W_j^s)\} + o_{\mathbb{P}}(1).$$

1080 Furthermore, we have

$$\sqrt{N_t}(\hat{\theta} - \theta_t) \Rightarrow \mathcal{N}(0, \sigma^2),$$

1082 so long as the asymptotic variance, given by

$$\sigma^2 = \text{Var}_t[\mu_0(W^t)] + \gamma \mathbb{E} [\alpha_0(W^s, C^s)^2 \text{Var}_s[Y^s | W^s]],$$

1085 is non-zero.

1087 The following corollary shows that one can use the plug-in variance estimate to construct asymptotically valid confidence intervals.

1089 **Corollary B.3.** *Under the same assumptions of Theorem B.2, the plug-in variance estimate*

$$\hat{\sigma}^2 := \mathbb{P}_{N_t} \left\{ \hat{\mu}(W^t, \hat{Y}^t) - \bar{\mu} \right\}^2 + \frac{N_t}{N_s} \mathbb{P}_{N_s} \hat{\alpha}(W^s, C^s)^2 \{Y^s - \hat{\mu}(W^s)\}^2$$

1093 is consistent, where $\bar{\mu} := \sum_{i=1}^{N_t} \hat{\mu}(W^t, \hat{Y}^t)$. Consequently, if the asymptotic variance σ^2 is non-zero, we have

$$\frac{\sqrt{N_t}}{\hat{\sigma}}(\hat{\theta} - \theta_t) \Rightarrow \mathcal{N}(0, 1),$$

1096 and thus

$$C_{1-\delta} := \left[\hat{\theta} - \frac{\hat{\sigma}}{\sqrt{N_t}} z_{\delta/2}, \hat{\theta} + \frac{\hat{\sigma}}{\sqrt{N_t}} z_{\delta/2} \right]$$

1101 is a $1 - \delta$ confidence interval for θ_t , where z_δ denotes the δ quantile of a standard normal random variable.

1103 The proofs of Theorem B.2 and Corollary B.3 follow immediately from applying Theorem C.1
1104 and Corollary C.3 in Appendix C (which concerns the case of general M-estimation) to the score
1105 $m(w, y; \theta) := y - \theta$.

1107 B.4 CROSS-FITTING FOR MEANS

1109 We now provide a cross-fitting algorithm for estimating $\theta_t = \mathbb{E}_t[Y]$ and state an analogue of Theorem B.2. In short, cross-fitting works by splitting the data in K folds of roughly equal size. If \mathcal{I}_k denotes the k th fold of data, the algorithm uses all data *outside* the k th fold (so, in the complement set \mathcal{I}_k^c) to construct nuisance estimates. These nuisance estimates are then used to estimate the mean on the k th fold. This splitting strategy ensures that, on each fold, the nuisance estimates and transformed data are independent of one another. This allows one to apply the asymptotic linearity result of Theorem B.2 on each fold to asymptotic normality of the cross-fitting estimate.

1116 We now state the cross-fitting algorithm (Algorithm 2) and corresponding convergence theorem
1117 (Theorem B.4). The proof of the cross-fitting result follows from Theorem C.4 in Appendix C, a
1118 generic result on cross-fitting for M-estimators under sampling bias.

1119 **Theorem B.4.** *Assume the same setup as Theorem B.2, and let $\hat{\mu}^{(-k)}, \hat{\alpha}^{(-k)}, \hat{\theta}$, and $\hat{\sigma}$ be as in
1120 Algorithm 2. Further, suppose the second assumption of Theorem B.2 holds for each nuisance
1121 estimate $\hat{\mu}^{(-1)}, \dots, \hat{\mu}^{(-K)}$ and $\hat{\alpha}^{(-1)}, \dots, \hat{\alpha}^{(-K)}$. Then, we have*

$$\frac{\sqrt{N_t}}{\hat{\sigma}}(\hat{\theta} - \theta_t) \Rightarrow \mathcal{N}(0, 1).$$

1125 Thus, the set $C_{1-\delta}$ defined in Corollary B.3 still serves as a $1 - \delta$ asymptotic confidence interval for
1126 θ_t .

1127
1128
1129
1130
1131
1132
1133

1134 **Algorithm 2** Doubly-Robust Estimator with K -fold Cross-Fitting (detailed version of Algorithm 1)

1135

1136 1: **Input:** Samples $\mathcal{D}_s := \{Z_1^s, \dots, Z_{N_s}^s\}$ from P_s , samples $\mathcal{D}_t := \{Z_1^t, \dots, Z_{N_t}^t\}$ from P_t ,
1137 number of folds K .

1138 2: Randomly split source indices $[N_s]$ into random folds of equal size: $\mathcal{I}_1, \dots, \mathcal{I}_K$.

1139 3: **for** $k \in [K]$ **do**

1140 4: Produce ML regression estimate $\hat{\mu}^{(-k)}$ using $\mathcal{D}_{s,k}^c$, where $\mathcal{D}_{s,k} := (Z_i^s : i \in \mathcal{I}_k)$.

1141 5: Produce ML nuisance estimate $\hat{\alpha}^{(-k)}$ using $\mathcal{D}_{s,k}^c$ and \mathcal{D}_t .

1142 6: Produce parameter and variance estimates:

1143
$$\hat{\theta}_k := \frac{1}{N_t} \sum_{i=1}^{N_t} \hat{\mu}^{(-k)}(W_i^t, \hat{Y}_i^t)$$

1144
$$+ \frac{K}{N_s} \sum_{j \in \mathcal{I}_k} \hat{\alpha}^{(-k)}(W_j^s, C_j^s) \left\{ Y_j^s - \hat{\mu}^{(-k)}(W_j^s, \hat{Y}_j^s) \right\},$$

1145

1146
$$\hat{\sigma}_k^2 := \frac{1}{N_t} \sum_{i=1}^{N_t} \left\{ \hat{\mu}^{(-k)}(W_i^t, \hat{Y}_i^t) - \hat{\theta}_k \right\}^2$$

1147

1148
$$+ \frac{N_t}{N_s} \frac{K}{N_s} \sum_{j \in \mathcal{I}_k} \hat{\alpha}^{(-k)}(W_j^s, C_j^s)^2 \left\{ Y_j^s - \hat{\mu}^{(-k)}(W_j^s, \hat{Y}_j^s) \right\}^2,$$

1149

1150

1151

1152

1153

1154 where $\hat{\theta}_k := \frac{1}{N_t} \sum_{i=1}^{N_t} \hat{\mu}^{(-k)}(W_i^t, \hat{Y}_i^t)$.

1155 7: Compute the average of the K estimates: $\hat{\theta} := \frac{1}{K} \sum_{k=1}^K \hat{\theta}_k$ and $\hat{\sigma}^2 := \frac{1}{K} \sum_{k=1}^K \hat{\sigma}_k^2$.

1156 8: **Return:** Mean estimate $\hat{\theta}$ and variance estimate $\hat{\sigma}^2$.

C GENERAL M-ESTIMATORS UNDER COVARIATE SHIFT

In this appendix, we prove a general result on the convergence of de-biased M-estimators under covariate and differential non-compliance. Our results from the previous appendix, which regarded the special case where the target parameter was the expected outcome $\theta_t = \mathbb{E}_t[Y]$, follow as a special case of the following.

Theorem C.1. Suppose Assumption 1 holds, and assume the learner has access to mutually independent samples $Z_1^s, \dots, Z_{N_s}^s$ from P_s and $Z_1^t, \dots, Z_{N_t}^t$ from P_t , as outlined in Assumption 2. Let $\psi_0(w)$ and $\alpha_0(w, c)$ be the true, unknown nuisances given by

$$\psi_0(w) := \mathbb{E}^t[m(W^t, Y^t; \theta_t) \mid W^t = w] \quad \text{and} \quad \alpha_0(w, c) = \frac{\omega_0(w)}{\pi_0(w)} c,$$

where $\pi_0(w) := P^s(C^s = 1 \mid W^s = w)$ and $\omega_0(w) := \frac{dP^t}{dP^s}(w)$. Suppose the following conditions hold.

1. (Ratio of Sample Sizes) There is some constant $0 < \gamma < \infty$ such that $N_t/N_s \rightarrow \gamma$.
2. (Nuisance Convergence) We have access to estimates $\hat{\psi}, \hat{\alpha}$ that are independent of the sample such that

$$\|\hat{\psi} - \psi_0\|_{L^2(P_Z^b)}, \|\hat{\alpha} - \alpha_0\|_{L^2(P_Z^b)} = o_{\mathbb{P}}(1)$$

and

$$\|\hat{\mu} - \mu_0\|_{L^2(P_Z^b)} \cdot \|\hat{\alpha} - \alpha_0\|_{L^2(P_Z^b)} = o_{\mathbb{P}}(N_t^{-1/2})$$

for $b \in \{s, t\}$. Further, we assume $\hat{\alpha}(w, 0) = 0$.

3. (Boundedness) The representer $\alpha_0(W^s, C^s)$ is almost surely bounded.
4. (Score Regularity) The score $m(w, y; \theta)$ satisfies the following regularity conditions:
 - (a) (Continuity) $m(w, y; \cdot) : \Theta \rightarrow \mathbb{R}^d$ is defined and continuous on a compact subset $\Theta \subset \mathbb{R}^d$.

1188 (b) (Unique Solution) There is a unique solution $\theta_t \in \mathbb{R}^d$ to equation $0 = \mathbb{E}_t[m(W^t, Y^t; \theta_t)]$. Further, $\theta_t \in \Theta^{int}$.⁶
 1189 (c) (Jacobian) The score $m(w, y; \theta)$ is continuously differentiable with respect to θ , and
 1190 the Jacobian $J_0 := \mathbb{E}_t[\nabla_\theta m(W^t, Y^t; \theta_t)]$ is non-singular.
 1191 (d) (Boundedness) We have
 1192

1193
$$\sup_{\theta, w, y} \|m(w, y; \theta)\|_2, \sup_{\theta, w, y} \|\nabla_\theta m(w, y; \theta)\|_{op} \leq D,$$

 1194

1195 for some universal constant $D > 0$.
 1196

1197 Let $\hat{\theta}$ be defined as the solution to the empirical estimating equation:

1198
$$0 = \mathbb{P}_{N_t} \hat{\psi}(W_i^t, \hat{Y}_i^t) + \mathbb{P}_{N_s} \hat{\alpha}(W_j^s, C_j^s) \left\{ m(W_j^s, Y_j^s; \hat{\theta}) - \hat{\psi}(W_j^s, \hat{Y}_j^s) \right\}. \quad (6)$$

 1199

1200 Then, we have asymptotic linearity:
 1201

1202
$$\sqrt{N_t}(\hat{\theta} - \theta_t) = \frac{-1}{\sqrt{N_t}} J_0^{-1} \left[\sum_{i=1}^{N_t} \psi_0(W^t) + \gamma \sum_{j=1}^{N_s} \alpha_0(W^s, C^s) \{m(W^s, Y^s; \theta_t) - \psi_0(W^s)\} \right] + o_{\mathbb{P}}(1).$$

 1203

1204 Consequently, we have that
 1205

1206
$$\sqrt{N_t}(\hat{\theta} - \theta_t) \Rightarrow \mathcal{N}(0, \Sigma_0),$$

 1207

1208 so long as the asymptotic variance, given by
 1209

1210
$$\Sigma_0 = J_0^{-1} \left(\text{Var}_t[\psi_0(W^t)] + \gamma \mathbb{E}_s [\alpha_0(W^s, C^s)^2 \text{Var}(m(W^s, Y^s; \theta_t) \mid W^s)] \right) J_0^{-T},$$

 1211

1212 is positive definite.
 1213

1214 Remark C.2. Many statistical parameters of interest can be specified via M-estimation problems.
 1215 We consider three relevant examples below.
 1216

1217 1. First, if we are interested in the mean outcome $\theta_t = \mathbb{E}_t[Y]$ (which was the focus of the
 1218 previous appendix), this can be trivially specified via the estimating equation:

1219
$$m(w, y; \theta) := y - \theta.$$

 1220

1221 Thus, the contributions of this appendix serve as a strict generalization of the results in
 1222 Appendix B.
 1223

1224 2. Next, suppose we are interested in the variance of responses under the target distribution,
 1225 i.e. $\theta_t := \text{Var}_t[Y] := \mathbb{E}_t[(Y - \mathbb{E}_t[Y])^2]$. Then, we can define the stacked estimating
 1226 equation

1227
$$m(w, y; (\rho, \theta)) := \begin{pmatrix} y - \rho \\ (y - \rho)^2 - \theta \end{pmatrix}.$$

 1228

1229 If $\eta_t := (\rho_t, \theta_t)$ denotes the solution to $0 = \mathbb{E}_t[m(W^s, Y^s; \eta_t)]$, we note that $\rho_t = \mathbb{E}_t[Y]$
 1230 and consequently $\theta_t = \text{Var}_t[Y]$.
 1231

1232 3. Lastly, suppose $Q \in (0, 1)$ and that we are interested in performing inference on the Q th
 1233 quantile of Y under P_t , i.e. $\theta_t := F_{Y,t}^{-1}(Q)$ where $F_{Y,t}(x) := P_t(Y \leq x)$ denotes the CDF
 1234 of Y under the target distribution, which we assume is invertible. Define the estimating
 1235 equation

1236
$$m(w, y; \theta) := Q - \mathbb{1}\{y \leq \theta\}.$$

 1237

1238 Then, one can check $0 = \mathbb{E}[m(W, Y; \theta_t)]$ by definition of the Q th quantile.
 1239

1240 We also note that, in the aforementioned examples, the M-estimators only depend on observed
 1241 outcomes Y and not the extended set of covariates W . While this is typically the case for most
 1242 parameters of interest, we allow m to depend on W for the sake of generality.
 1243

1244 ⁶Here, Θ^{int} denotes the interior of Θ , i.e. the largest open set contained in Θ

The following corollary shows how one can use the above result to construct asymptotically-valid confidence intervals. This is accomplished by normalizing the parameter estimate $\widehat{\theta}$ by the square root the classic “sandwich” variance estimator. The consistency of this estimator follows from standard proof techniques (see Van der Vaart (2000); Chernozhukov et al. (2018)). With the consistency the variance estimate, the result then follows from an application of the continuous mapping theorem.

Corollary C.3. *Define the plug-in “sandwich” variance estimator as*

$$\widehat{\Sigma} := \widehat{J}^{-1} \widehat{V} \widehat{J}^{-T},$$

where \widehat{V} and \widehat{J} are respectively defined as

$$\begin{aligned} \widehat{V} &= \frac{1}{N_t} \sum_{i=1}^{N_t} \widehat{\psi}(W^t, \widehat{Y}^t)^{\otimes 2} + \frac{N_t}{N_s} \frac{1}{N_s} \sum_{j=1}^{N_s} \widehat{\alpha}(W^s, C^s)^2 \left\{ m(W^s, \widehat{Y}^s; \widehat{\theta}) - \widehat{\psi}_0(W^s, \widehat{Y}^s) \right\}^{\otimes 2} \\ \widehat{J} &:= \frac{1}{N_s} \sum_{i=1}^{N_s} \widehat{\alpha}(W^s, C^s) \nabla_{\theta} m(W^s, Y^s; \widehat{\theta}). \end{aligned}$$

Then, under the same assumptions of Theorem C.1, $\widehat{\Sigma}$ is consistent, and hence

$$\sqrt{N_t} \widehat{\Sigma}^{-1/2} (\widehat{\theta} - \theta_0) \Rightarrow \mathcal{N}(0, I_d).$$

Thus, for any fixed unit vector $\nu \in \mathbb{R}^d$, the set

$$C_{1-\delta} := \left[\nu^{\top} \widehat{\theta} - \sqrt{\frac{\nu^{\top} \widehat{\Sigma} \nu}{N_t}} z_{\delta/2}, \nu^{\top} \widehat{\theta} + \sqrt{\frac{\nu^{\top} \widehat{\Sigma} \nu}{N_t}} z_{\delta/2} \right]$$

forms a $1 - \delta$ confidence interval for $\nu^{\top} \theta_t$.

C.1 CROSS-FITTING FOR M-ESTIMATORS

As in Appendix B, we provide a cross-fitting algorithm that allows the learner to make more efficient use of the available data. We also state a corresponding convergence theorem (an analogue of Theorem B.4), whose proof follows from applying the asymptotic linearity of estimators on each fold.

Theorem C.4. *Assume the same setup as Theorem C.1, and suppose $\widehat{\psi}^{(-k)}, \widehat{\alpha}^{(-k)}, \widehat{\theta}$, and $\widehat{\Sigma}$ are as in Algorithm 3. Further, suppose the second Assumption of Theorem C.1 holds for each nuisance estimate $\widehat{\psi}^{(-1)}, \dots, \widehat{\psi}^{(-K)}$ and $\widehat{\alpha}^{(-1)}, \dots, \widehat{\alpha}^{(-K)}$. Then, we have*

$$\sqrt{N_t} \widehat{\Sigma}^{-1/2} (\widehat{\theta} - \theta_t) \Rightarrow \mathcal{N}(0, I_d).$$

Thus, the set $C_{1-\delta}$ defined in Corollary C.3 still serves as a $1 - \delta$ asymptotic confidence interval for θ_t .

Proof. First, we know from Theorem C.1 that

$$\begin{aligned} \widehat{\theta}_k - \theta_t &= \frac{-1}{N_t} J_0^{-1} \sum_{i=1}^{N_t} \psi_0(W_i^t) \\ &\quad - J_0^{-1} \frac{K\gamma}{N_t} \sum_{j \in \mathcal{I}_k} \alpha_0(W_j^s, C_j^s) \{m(W_j^s, Y_j^s; \theta_t) - \psi_0(W_j^s)\} + o_{\mathbb{P}}(N_t^{-1/2}). \end{aligned}$$

Consequently, we have

$$\begin{aligned} \widehat{\theta} - \theta_t &= \frac{1}{K} \sum_{k=1}^K (\widehat{\theta}_k - \theta_t) \\ &= \frac{1}{K} \sum_{k=1}^K \frac{1}{N_t} J_0^{-1} \left[\sum_{i=1}^{N_t} \psi_0(W_i^t) + K \gamma \sum_{j \in \mathcal{I}_k} \alpha_0(W_j^s, C_j^s) \{m(W_j^s, Y_j^s; \theta_t) - \psi_0(W_j^s)\} \right] + o_{\mathbb{P}}(N_t^{-1/2}) \\ &= \frac{1}{N_t} J_0^{-1} \left[\sum_{i=1}^{N_t} \psi_0(W_i^t) + \gamma \sum_{j=1}^N \alpha_0(W_j^s, C_j^s) \{m(W_j^s, Y_j^s; \theta_t) - \psi_0(W_j^s)\} \right] + o_{\mathbb{P}}(N_t^{-1/2}) \end{aligned}$$

1296 **Algorithm 3** Doubly-Robust M-Estimation with K -fold Cross-Fitting

1297 1: **Input:** Samples $\mathcal{D}_s := \{Z_1^s, \dots, Z_{N_s}^s\}$ from P_s , samples $\mathcal{D}_t := \{Z_1^t, \dots, Z_{N_t}^t\}$ from P_t ,
 1298 number of folds K .
 1299 2: Randomly split source indices $[N_s]$ random folds of equal size: $\mathcal{I}_1, \dots, \mathcal{I}_K$.
 1300 3: **for** $k \in [K]$ **do**
 1301 4: Produce ML regression estimate $\hat{\psi}^{(-k)}$ using $\mathcal{D}_{s,k}^c$, where $\mathcal{D}_{s,k} := (Z_i^s : i \in \mathcal{I}_k)$.
 1302 5: Produce ML nuisance estimate $\hat{\alpha}^{(-k)}$ using $\mathcal{D}_{s,k}^c$ and \mathcal{D}_t .
 1303 6: Let $\hat{\theta}^{(k)}$ solve Equation (6), i.e.
 1304
 1305
$$0 = \frac{1}{N_t} \sum_{i=1}^{N_t} \hat{\psi}^{(-k)}(W_i^t, \hat{Y}_i^t)$$

 1306
$$+ \frac{K}{N_s} \sum_{j \in \mathcal{I}_k} \hat{\alpha}^{(-k)}(W_j^s, C_j^s) \left\{ m(W_j^s, Y_j^s; \hat{\theta}_k) - \hat{\psi}^{(-k)}(W_j^s, \hat{Y}_j^s) \right\}.$$

 1307
 1308 7: Let \hat{J}_k , \hat{V}_k , and $\hat{\Sigma}_k$ be given as
 1309
 1310
$$\hat{J}_k := \frac{K}{N_s} \sum_{j \in \mathcal{I}_k} \hat{\alpha}^{(-k)}(W_j^s, C_j^s) \nabla_{\theta} m(W_j^s, Y_j^s; \hat{\theta}_k),$$

 1311
 1312
$$\hat{V}_k := \frac{1}{N_t} \sum_{i=1}^{N_t} \hat{\psi}^{(-k)}(W_i^t, \hat{Y}_i^t)^{\otimes 2}$$

 1313
$$+ \frac{N_t}{N_s} \frac{K}{N_s} \sum_{j \in \mathcal{I}_k} \hat{\alpha}^{(-k)}(W_j^s, C_j^s)^2 \left\{ m(W_j^s, Y_j^s; \hat{\theta}_k) - \hat{\psi}^{(-k)}(W_j^s, \hat{Y}_j^s) \right\}^{\otimes 2},$$

 1314
 1315
$$\hat{\Sigma}_k := \hat{J}_k^{-1} \hat{V}_k \hat{J}_k^{-T}.$$

 1316
 1317 8: Compute the average of the K estimates: $\hat{\theta} := \frac{1}{K} \sum_{k=1}^K \hat{\theta}_k$ and $\hat{\Sigma} := \frac{1}{K} \sum_{k=1}^K \hat{\Sigma}_k$.
 1318 9: **Return:** Estimate $\hat{\theta}$ and variance estimate $\hat{\Sigma}$.

1326
 1327
 1328
 1329
 1330 The result that $\sqrt{N_t}(\hat{\theta} - \theta_t) \Rightarrow \mathcal{N}(0, \Sigma_0)$ follows immediately from the above asymptotic linearity.

1331 Next, observe that Corollary C.3 yields that, for each $k \in [K]$, the variance estimate $\hat{\Sigma}_k$ is consistent
 1332 for Σ_0 , i.e. that we have $\hat{\Sigma}_k = \Sigma_0 + o_{\mathbb{P}}(1)$, and consequently we have $\hat{\Sigma} := \frac{1}{K} \sum_{k=1}^K \hat{\Sigma}_k =$
 1333 $\frac{1}{K} \sum_{k=1}^K \{\Sigma_0 + o_{\mathbb{P}}(1)\} = \Sigma + o_{\mathbb{P}}(1)$. Thus, we have the consistency of the cross-fit variance
 1334 estimate. Since $\Sigma_0 \succ 0$, which follows from non-singularity of J_0 and V_t , the continuous mapping
 1335 theorem also implies that $\hat{\Sigma}^{-1/2} - \Sigma_0^{-1/2} = o_{\mathbb{P}}(1)$. As a consequence, we have
 1336

1337
 1338
 1339
 1340
$$\hat{\Sigma}^{-1/2}(\hat{\theta} - \theta_t) = \Sigma_0^{-1/2}(\hat{\theta} - \theta_t) + \left(\hat{\Sigma}^{-1/2} - \Sigma_0^{-1/2} \right) (\hat{\theta} - \theta_t)$$

 1341
 1342
$$= \Sigma_0^{-1/2}(\hat{\theta} - \theta_t) + o_{\mathbb{P}}(1) \cdot O_{\mathbb{P}}(N_t^{-1/2})$$

 1343
 1344
$$= \Sigma_0^{-1/2} \frac{1}{N_t} J_0^{-1} \left[\sum_{i=1}^{N_t} \psi_0(W_i^t) + \gamma \sum_{j=1}^N \alpha_0(W_j^s, C_j^s) \{m(W_j^s, Y_j^s; \theta_t) - \psi_0(W_j^s)\} \right] + o_{\mathbb{P}}(N_t^{-1/2}).$$

 1345
 1346
 1347
 1348
 1349

In particular, this implies $\sqrt{N_t} \hat{\Sigma}^{-1/2}(\hat{\theta} - \theta_t) \Rightarrow \mathcal{N}(0, 1)$, proving the other claim. \square

1350 C.2 PROOF OF THEOREM C.1
13511352 *Proof.* Observe that, by the definition of $\hat{\theta}$, we have the identity
1353

1354
$$0 = \mathbb{P}_{N_t} \hat{\psi}(W^t, \hat{Y}^t) + \mathbb{P}_{N_s} \left\{ \hat{\alpha}(W^s, C^s)(m(W^s, Y^s; \hat{\theta}) - \hat{\psi}(W^s, \hat{Y}^s)) \right\}$$

1355
1356
$$= \mathbb{P}_{N_t} \hat{\psi}(W^t, \hat{Y}^t) + \mathbb{P}_{N_s} \left\{ \hat{\alpha}(W^s, C^s)(m(W^s, Y^s; \theta_0) - \hat{\psi}(W^s, \hat{Y}^s)) \right\}$$

1357
1358
$$+ \mathbb{P}_{N_s} \left\{ \hat{\alpha}(W^s, C^s) \nabla_{\theta} m(W^s, Y^s; \hat{\theta})(\hat{\theta} - \theta_t) \right\},$$

1359 where the second equality follows from performing a first-order Taylor expansion with mean-value
1360 theorem remainder and $\hat{\theta} \in [\theta_t, \hat{\theta}]$, which we are able to apply since $m(w, y; \theta)$ is assumed to
1361 be continuously differentiable (this implies $\mathbb{P}_{N_s} \{\hat{\alpha}(W^s, C^s)m(W^s, Y^s; \theta)\}$ is also continuously
1362 differentiable w.r.t. θ). Rearranging the above expression, we arrive at
1363

1364
$$\sqrt{N_t}(\hat{\theta} - \theta_t) = -\sqrt{N_t} \underbrace{\left(\mathbb{P}_{N_s} \hat{\alpha}(W^s, C^s) \nabla_{\theta} m(W^s, Y^s; \hat{\theta}) \right)^{-1}}_{T_1}$$

1365
1366
$$\times \underbrace{\left[\mathbb{P}_{N_t} \hat{\psi}(W^t, \hat{Y}^t) + \mathbb{P}_{N_s} \left\{ \hat{\alpha}(W^s, C^s)(m(W^s, Y^s; \theta_t) - \hat{\psi}(W^s, \hat{Y}^s)) \right\} \right]}_{T_2}.$$

1367
1368
1369

1370 To prove the desired asymptotic linearity result, we need to show two things.
13711372 1. We must show that T_1 converges in probability to the true Jacobian, i.e. that $T_1 = J_0^{-1} +$
1373 $o_{\mathbb{P}}(1)$.
1374
1375 2. Next, we need to show that

1376
$$T_2 = \mathbb{P}_{N_t} \psi_0(W^t) + \mathbb{P}_{N_s} \alpha_0(W^s, C^s) \{m(W^s, Y^s; \theta_t) - \psi_0(W^s)\} + o_{\mathbb{P}}(N_t^{-1/2})$$

1377
1378

1379 After we have shown both desiderata above to be true, we can piece the result together. In particular,
1380 we have
1381

1382
$$\begin{aligned} \sqrt{N_t}(\hat{\theta} - \theta_t) &= -\sqrt{N_t}(J_0^{-1} + o_{\mathbb{P}}(1)) \\ 1383 &\times \left[\mathbb{P}_{N_t} \psi_0(W^t) + \mathbb{P}_{N_s} \alpha_0(W^s, C^s) \{m(W^s, Y^s; \theta_t) - \psi_0(W^s)\} + o_{\mathbb{P}}(N_t^{-1/2}) \right] \\ 1384 &= \frac{-1}{\sqrt{N_t}} \sum_{i=1}^{N_t} J_0^{-1} \psi_0(W^t) + \frac{-\gamma}{\sqrt{N_t}} \sum_{j=1}^{N_s} J_0^{-1} \{\alpha_0(W^s, C^s)(m(W^s, Y^s; \theta_t) - \psi_0(W^s))\} + o_{\mathbb{P}}(1), \end{aligned}$$

1385
1386

1387 which provides the desired asymptotic linearity result. Asymptotic normality now follows immediately
1388 from the above.
13891390 **Analyzing T_2 :** First, we argue that T_2 is asymptotically linear. To do this, we primarily follow the
1391 proof of Theorem 1 in Chernozhukov et al. (2023). For notational ease, let $M^s := m(W^s, Y^s; \theta_0)$.
1392 We can rewrite T_2 as
1393

1394
$$T_2 = \mathbb{P}_{N_t} \psi_0(W^t) + \mathbb{P}_{N_s} \alpha_0(W^s, C^s) \{M^s - \psi_0(W^s)\} + R_1 + R_2 + R_3,$$

1395

1396 where (letting $\psi_0(w, \hat{y}) := \psi_0(w)$)
1397

1398
$$\begin{aligned} R_1 &= \mathbb{P}_{N_t} \left\{ (\hat{\psi} - \psi_0)(W^s, \hat{Y}^s) \right\} + \mathbb{P}_{N_s} \left\{ \alpha_0(W^s, C^s)(\psi_0 - \hat{\psi})(W^s, \hat{Y}^s) \right\} \\ 1399 R_2 &= \mathbb{P}_{N_s} \left\{ (\hat{\alpha} - \alpha_0)(W^s, C^s)(M^s - \psi_0(W^s)) \right\} \\ 1400 R_3 &= \mathbb{P}_{N_s} \left\{ (\hat{\alpha} - \alpha_0)(W^s, C^s)(\psi_0 - \hat{\psi})(W^s, \hat{Y}^s) \right\}. \end{aligned}$$

1401

1402 We show that $R_1, R_2, R_3 = o_{\mathbb{P}}(N_t^{-1/2})$ (or equivalently that the above terms are
1403 $o_{\mathbb{P}}(N_s^{-1/2})$ since $N_s = \Theta(N_t)$ by assumption). Since $\mathbb{E}_Z^t [(\hat{\psi} - \psi_0)(W^s, \hat{Y}^s)] =$

1404 $\mathbb{E}_Z^s \left[\alpha_0(W^s, C^s)(\psi_0 - \hat{\psi})(W^s, \hat{Y}^s) \right]$ by Lemma B.1, we have
1405

$$1406 R_1 = \underbrace{(\mathbb{P}_{N_t} - \mathbb{E}_Z^t) \left\{ (\hat{\psi} - \psi_0)(W^t, \hat{Y}^t) \right\}}_{R'_1} + \underbrace{(\mathbb{P}_{N_s} - \mathbb{E}_Z^s) \left\{ \alpha_0(W^s, C^s)(\psi_0 - \hat{\psi})(W^s, \hat{Y}^s) \right\}}_{R''_1}.$$

1409 Using the same steps from in the proof of Theorem 1 of Chernozhukov et al. (2023) and letting
1410 $(\hat{\psi} - \psi_0)_k$ denote the k component of $\hat{\psi} - \psi_0$, we have
1411

$$\begin{aligned} 1412 \mathbb{E}_Z^t \|R'_1\|_2^2 &= \sum_{k=1}^d \mathbb{E}_Z^t \left((\mathbb{P}_{N_t} - \mathbb{E}_Z^t)(\hat{\psi} - \psi_0)_k (W^s, \hat{Y}^s)^2 \right) \\ 1413 &= \frac{1}{N_t} \sum_{k=1}^d \text{Var}_Z^t \left[(\hat{\psi} - \psi_0)_k (W^s, \hat{Y}^s) \right] \\ 1414 &\leq \frac{1}{N_t} \sum_{k=1}^d \mathbb{E}_Z^t \left((\hat{\psi} - \psi_0)_k (W^s, \hat{Y}^s)^2 \right) && \text{(Since } \text{Var}[X] \leq \mathbb{E}X^2) \\ 1415 &= \frac{1}{N_t} \|\hat{\psi} - \psi_0\|_{L^2(P_Z^t)}. \\ 1416 \end{aligned}$$

1417 Thus, for any $\epsilon > 0$, we have, via an application of the tower rule and Chebyshev's inequality,
1418

$$\begin{aligned} 1419 P_t(N_t^{1/2} \|R'_1\|_2 \geq \epsilon) &= \mathbb{E}_t \left[P_Z^t(N_t^{1/2} \|R'_1\|_2 \geq \epsilon) \right] \\ 1420 &\leq \frac{1}{\epsilon^2} \mathbb{E}_t \left[\|\hat{\psi} - \psi_0\|_{L^2(P_Z^t)}^2 \right] = o(1), \\ 1421 \end{aligned}$$

1422 where the final equality follows since $\|\hat{\psi} - \psi_0\|_{L^2(P_Z^t)} = o_{\mathbb{P}}(1)$ and $\|\hat{\psi} - \psi_0\|_{L^\infty(P_Z^t)} = O(1)$ imply
1423 $\lim_{n \rightarrow \infty} \mathbb{E}_t \|\hat{\psi} - \psi_0\|_{L^2(P^t)} = 0$. Thus, since $\epsilon > 0$ was arbitrary, $R'_1 = o_{\mathbb{P}}(N_t^{-1/2})$.
1424

1425 Next, since $\|\alpha_0\|_{L^\infty(P_Z^s)} = O(1)$, an analogous argument yields that
1426

$$\mathbb{E}_Z^s \|R''_1\|_2^2 \leq \frac{1}{N_s} \|\hat{\psi} - \psi_0\|_{L^2(P_Z^s)},$$

1427 and thus working through the same argument involving conditionally applying Chebyshev's inequality
1428 yields $R''_1 = o_{\mathbb{P}}(N_s^{-1/2})$, which in turn shows $R_1 = o_{\mathbb{P}}(N_s^{-1/2}) = o_{\mathbb{P}}(N_t^{-1/2})$.
1429

1430 Next, we bound R_2 . Again we start by bounding the conditional expectation of the norm of R_2 given
1431 $\hat{\alpha}$. Since $\|\text{Cov}(m(X^s, Y^s; \theta_0) \mid W^s)\|_{op} = O(1)$ by the assumption that $m(x, y; \theta)$ is bounded, we
1432 have
1433

$$\begin{aligned} 1434 \mathbb{E}_Z^s \|R_2\|_2^2 &= \sum_{k=1}^d \mathbb{E}_Z^s \left(\{\mathbb{P}_{N_s}(\hat{\alpha} - \alpha_0)(W^s, C^s)(M_k^s - \psi_0(W^s)_k)\}^2 \right) \\ 1435 &= \frac{1}{N_s} \sum_{k=1}^d \mathbb{E}_Z^s \left(\mathbb{P}_{N_s} \{(\hat{\alpha} - \alpha_0)(W^s, C^s)^2 (M_k^s - \psi_0(W^s)_k)^2\} \right) \\ 1436 &= \frac{1}{N_s} \sum_{k=1}^d \mathbb{E}_Z^s ((\hat{\alpha} - \alpha_0)(W^s, C^s)^2 (M_k^s - \psi_0(W^s)_k)^2) \\ 1437 &= \frac{1}{N_s} \sum_{k=1}^d \mathbb{E}_Z^s ((\hat{\alpha} - \alpha_0)(W^s, C^s)^2 \text{Cov}_s(M_k^s \mid W^s)) \\ 1438 &\leq \frac{1}{N_s} \sup_w |\text{Tr}\{\text{Cov}_s(M^s \mid W^s = w)\}| \mathbb{E}_Z^s [(\hat{\alpha} - \alpha_0)(W^s, C^s)^2] \\ 1439 &\lesssim \frac{1}{N_s} \|\hat{\alpha} - \alpha_0\|_{L^2(P_Z^s)}^2. \\ 1440 \end{aligned}$$

1441 From this, we have again via applying Chebyshev's inequality conditionally that $R_2 = o_{\mathbb{P}}(N_s^{-1/2})$.
1442

1458 Finally, we bound R_3 . We have
 1459

$$\begin{aligned}
 1460 \mathbb{E}_Z^s \|R_3\|_2 &\leq \sum_{k=1}^d \mathbb{E}_Z^s |(\hat{\alpha} - \alpha_0)(W^s, C^s)(\psi_0 - \hat{\psi})_k(W^s, \hat{Y}^s)| && \text{(Since } \|x\|_2 \leq \|x\|_1\text{)} \\
 1461 &\leq \sum_{k=1}^d \|\hat{\alpha} - \alpha_0\|_{L^2(P_Z^s)} \|\hat{\psi}_k - \psi_{0,k}\|_{L^2(P_Z^s)} && \text{(Cauchy-Schwarz)} \\
 1462 &\leq \sqrt{d} \|\hat{\alpha} - \alpha_0\|_{L^2(P_Z^s)} \|\hat{\psi} - \psi_0\|_{L^2(P_Z^s)} = o_{\mathbb{P}}(N_s^{-1/2}),
 \end{aligned}$$

1463 where the final inequality follows because $\|x\|_1 \leq \sqrt{d}\|x\|_2$ and the final equality follows by
 1464 assumption on nuisance estimation rates. Conditionally applying Markov's inequality yields that
 1465 $R_3 = o_{\mathbb{P}}(N_s^{-1/2}) = o_{\mathbb{P}}(N_t^{-1/2})$, thus proving the desired asymptotic linearity result for T_2 .
 1466

1467 **Analyzing T_1 :** Next, we argue that $T_1 = J_{N_s}(\tilde{\theta}, \hat{\alpha}) \xrightarrow[N_s \rightarrow \infty]{\mathbb{P}} J(\theta_t, \alpha_0) \equiv J_0$, where for any $\theta \in \Theta$
 1468 and $\alpha \in L^2(P^s)$ we define:
 1469

$$\begin{aligned}
 1470 J(\theta, \alpha) &:= \mathbb{E}_Z^s [\alpha(W^s, C^s) \nabla_\theta m(W^s, Y^s; \theta)] \in \mathbb{R}^{d \times d} \\
 1471 J_{N_s}(\theta, \alpha) &:= \mathbb{P}_{N_s} \{ \alpha(W^s, C^s) \nabla_\theta m(W^s, Y^s; \theta) \} \in \mathbb{R}^{d \times d}.
 \end{aligned}$$

1472 Throughout this part of the proof, we assume that $\hat{\theta}$ is a consistent estimate of θ_t , i.e. that $\|\hat{\theta} - \theta_t\|_2 =$
 1473 $o_{\mathbb{P}}(1)$. We formally prove this in sequel. Note we can write
 1474

$$\|T_1 - J(\theta_t, \alpha_0)\|_{op} \leq \underbrace{\|J_{N_s}(\tilde{\theta}, \hat{\alpha}) - J(\tilde{\theta}, \hat{\alpha})\|_{op}}_{R_1} + \underbrace{\|J(\tilde{\theta}, \hat{\alpha}) - J(\tilde{\theta}, \alpha_0)\|_{op}}_{R_2} + \underbrace{\|J(\tilde{\theta}, \alpha_0) - J(\theta_t, \alpha_0)\|_{op}}_{R_3}.$$

1475 We show $R_1, R_2, R_3 = o_{\mathbb{P}}(1)$, which suffices to prove the result.
 1476

1477 To show $R_1 = o_{\mathbb{P}}(1)$, it suffices to show that $\sup_{\theta \in \Theta} \|J_{N_s}(\theta, \hat{\alpha}) - J(\theta, \hat{\alpha})\|_{op} = o_{\mathbb{P}}(1)$. We
 1478 know that for any fixed square-integrable function $\alpha(w, c)$, since $\nabla_\theta m(w, y; \theta)$ is bounded above in
 1479 operator norm by some constant D , we have $\|\alpha(w, c) \nabla_\theta m(w, y; \theta)\|_{op} \leq D|\alpha(w, c)|$, and so the
 1480 collection of scores possesses an integrable envelope. Further, since $\nabla_\theta m(w, y; \theta)$ is continuous in
 1481 θ , the score $\alpha(w, c) \nabla_\theta m(w, y; \theta)$ is continuous as well. Lastly, since Θ is compact, Lemma 2.4 of
 1482 Newey & McFadden (1994) yields that $\{\alpha(w, c) \nabla_\theta m(w, y; \theta) : \theta \in \Theta\}$ is a weak Glivenko-Cantelli
 1483 class, i.e. that
 1484

$$\sup_{\theta} \|J_{N_s}(\theta, \alpha) - J(\theta, \alpha)\|_{op} = o_{\mathbb{P}}(1). \quad (7)$$

1485 Since $\hat{\alpha}$ is independent of Z_1^s, \dots, Z_N^s and bounded, we get for any $\epsilon > 0$
 1486

$$\begin{aligned}
 1487 \lim_{N_s \rightarrow \infty} P_s \left(\sup_{\theta} \|J_{N_s}(\theta, \hat{\alpha}) - J(\theta, \hat{\alpha})\|_{op} > \epsilon \right) &= \lim_{N_s \rightarrow \infty} \mathbb{E}_s \left[\underbrace{P_Z^s \left(\sup_{\theta} \|J_{N_s}(\theta, \hat{\alpha}) - J(\theta, \hat{\alpha})\|_{op} > \epsilon \right)}_{\phi_{N_s}(\hat{\alpha})} \right] \\
 1488 &= 0.
 \end{aligned}$$

1489 In the above, the final limit follows because $\lim_{N_s \rightarrow \infty} \phi_{N_s}(\hat{\alpha}) = 0$ by Equation (7), which allows
 1490 us to apply the bounded convergence theorem (see Chapter 1 of Durrett (2019)). Thus, we have
 1491 $\sup_{\theta} \|J_N(\theta, \hat{\alpha}) - J(\theta, \hat{\alpha})\|_{op} = o_{\mathbb{P}}(1)$.
 1492

1493 Next, we show $R_2 = o_{\mathbb{P}}(1)$. Again, it actually suffices to show that $\sup_{\theta \in \Theta} \|J(\theta, \hat{\alpha}) -$
 1494 $J(\theta, \alpha_0)\|_{op} = o_{\mathbb{P}}(1)$, which we now show. Observe that, for any fixed $\theta \in \Theta$, we have
 1495

$$\begin{aligned}
 1496 \|J(\theta, \hat{\alpha}) - J(\theta, \alpha_0)\|_{op} &= \|\mathbb{E}_Z^s [(\hat{\alpha} - \alpha_0)(W^s, C^s) \nabla_\theta m(W^s, Y^s; \theta)]\|_{op} \\
 1497 &\leq \mathbb{E}_Z^s \left[|(\hat{\alpha} - \alpha_0)(W^s, C^s)| \|\nabla_\theta m(W^s, Y^s; \theta)\|_{op} \right] \\
 1498 &\leq D \mathbb{E}_Z^s |(\hat{\alpha} - \alpha_0)(W^s, C^s)| \\
 1499 &\leq D \|\hat{\alpha} - \alpha_0\|_{L^2(P^s)} \\
 1500 &= o_{\mathbb{P}}(1) \quad (\text{Nuisance consistency}).
 \end{aligned}$$

1512 Lastly, we show that $R_3 = o_{\mathbb{P}}(1)$. This follows as we have
 1513

$$\begin{aligned} 1514 \quad R_3 &= \left\| \mathbb{E}_Z^s \left[\alpha_0(W^s, C^s) \left\{ \nabla_{\theta} m(W^s, Y^s; \tilde{\theta}) - \nabla_{\theta} m(W^s, Y^s; \theta_t) \right\} \right] \right\|_{op} \\ 1515 &\leq \|\alpha_0\|_{L^\infty(P_s)} \mathbb{E}_Z^s \left\| \nabla_{\theta} m(W^s, Y^s; \tilde{\theta}) - \nabla_{\theta} m(W^s, Y^s; \theta_t) \right\|_{op} \\ 1516 &= o_{\mathbb{P}}(1), \\ 1517 \end{aligned}$$

1519 where the final equality follows from the continuous mapping theorem and the fact that $\tilde{\theta}$ is
 1520 consistent for θ_0 . Since we have showed all three terms converge in probability to zero, we have that
 1521 $T_1 - J_0 \equiv J_n(\tilde{\theta}, \hat{\alpha}) - J(\theta_t, \alpha_0) = o_{\mathbb{P}}(1)$, proving the result.
 1522

1523 **Consistency of $\hat{\theta}$:** We now argue the consistency of $\hat{\theta}$. To do this, we first show that
 1524

$$1525 \quad \|\mathbb{P}_{N_t} \hat{\psi}(W^t, \hat{Y}^t)\|_2 = o_{\mathbb{P}}(1) \quad \text{and} \quad \|\mathbb{P}_{N_s} \hat{\alpha}(W^s, C^s) \hat{\psi}(W^s, \hat{Y}^s)\|_2 = o_{\mathbb{P}}(1). \quad (8)$$

1526 We just show the second quantity approaches zero in probability. Showing the former approaches
 1527 zero follows from a similar, simpler argument. We have
 1528

$$\begin{aligned} 1529 \quad \mathbb{P}_{N_s} \hat{\alpha}(W^s, C^s) \hat{\psi}(W^s, \hat{Y}^s) &= \underbrace{(\mathbb{P}_{N_s} - \mathbb{E}_Z^s) \left\{ \hat{\alpha}(W^s, C^s) \hat{\psi}(W^s, \hat{Y}^s) - \alpha_0(W^s, C^s) \psi_0(W^s) \right\}}_{R_1} \\ 1530 &+ \underbrace{(\mathbb{P}_{N_s} - \mathbb{E}_Z^s) \{ \alpha_0(W^s, C^s) \psi_0(W^s) \}}_{R_2} \\ 1531 &+ \underbrace{\mathbb{E}_Z^s \left[\hat{\alpha}(W^s, C^s) \hat{\psi}(W^s, \hat{Y}^s) - \alpha_0(W^s, C^s) \psi_0(W^s) \right]}_{R_3}, \\ 1532 \\ 1533 \\ 1534 \\ 1535 \\ 1536 \\ 1537 \end{aligned}$$

1538 which follows since $\mathbb{E}_Z^s [\alpha_0(W^s, C^s) \psi_0(W^s)] = 0$.

1539 Now, since α_0 and ψ_0 are almost surely bounded, we have $R_2 = o_{\mathbb{P}}(1)$ by the weak law of large
 1540 numbers. Next, we can show $R_1 = o_{\mathbb{P}}(1)$ by conditionally applying Chebyshev's inequality. In
 1541 particular, for any $\epsilon > 0$, we have
 1542

$$\begin{aligned} 1543 \quad P_s(\|R_1\| \geq \epsilon) &= \mathbb{E}_s [P_Z^s(\|R_1\| \geq \epsilon)] \\ 1544 &\leq \frac{1}{\epsilon^2} \mathbb{E}_s \left[\mathbb{E}_Z^s \left(\left\| (\mathbb{P}_{N_s} - \mathbb{E}_Z^s) \left\{ \hat{\alpha}(W^s, C^s) \hat{\psi}(W^s, \hat{Y}^s) - \alpha_0(W^s, C^s) \psi_0(W^s) \right\} \right\|_2^2 \right) \right] \\ 1545 &= \frac{1}{\epsilon^2} \mathbb{E}_s \left[\sum_{k=1}^d \mathbb{E}_Z^s \left[\left((\mathbb{P}_{N_s} - \mathbb{E}_Z^s) \left\{ \hat{\alpha}(W^s, C^s) \hat{\psi}(W^s, \hat{Y}^s)_k - \alpha_0(W^s, C^s) \psi_0(W^s)_k \right\} \right)^2 \right] \right] \\ 1546 &= \frac{1}{N_s \epsilon^2} \mathbb{E}_s \left[\sum_{k=1}^d \text{Var}_Z^s \left[\hat{\alpha}(W^s, C^s) \hat{\psi}(W^s, \hat{Y}^s)_k - \alpha_0(W^s, C^s) \psi_0(W^s)_k \right] \right] \\ 1547 &\leq \frac{1}{N_s \epsilon^2} \mathbb{E}_s \left[\sum_{k=1}^d \mathbb{E}_Z^s \left(\left\{ \hat{\alpha}(W^s, C^s) \hat{\psi}(W^s, \hat{Y}^s)_k - \alpha_0(W^s, C^s) \psi_0(W^s)_k \right\}^2 \right) \right] \\ 1548 &\lesssim \frac{1}{N_s \epsilon^2} \mathbb{E}_s \left[\sum_{k=1}^d \mathbb{E}_Z^s \left(\left\{ \hat{\alpha}(W^s, C^s) \hat{\psi}(W^s, \hat{Y}^s)_k - \alpha_0(W^s, C^s) \hat{\psi}(W^s, \hat{Y}^s)_k \right\}^2 \right) \right] \\ 1549 &\quad + \frac{1}{N_s \epsilon^2} \mathbb{E}_s \left[\sum_{k=1}^d \mathbb{E}_Z^s \left(\left\{ \alpha_0(W^s, C^s) \hat{\psi}(W^s, \hat{Y}^s)_k - \alpha_0(W^s, C^s) \psi_0(W^s)_k \right\}^2 \right) \right] \\ 1550 &\lesssim \frac{1}{N_s \epsilon^2} \left\{ \mathbb{E}_s [\|\hat{\alpha} - \alpha_0\|_{L^2(P_s)}] + \mathbb{E} [\|\hat{\psi} - \psi_0\|_{L^2(P_s)}] \right\} \\ 1551 &= o_{\mathbb{P}}(1), \\ 1552 \\ 1553 \\ 1554 \\ 1555 \\ 1556 \\ 1557 \\ 1558 \\ 1559 \\ 1560 \\ 1561 \\ 1562 \\ 1563 \\ 1564 \\ 1565 \end{aligned}$$

where the second to last inequality follows from the fact that $\text{Var}[X] \leq \mathbb{E}X^2$, the second to in-
 1566 equality follows from adding and subtracting $\alpha_0(W^s, C^s) \hat{\psi}(W^s, \hat{Y}^s)_k$, applying the parallelogram

1566 inequality, and the final inequality follows from the boundedness of nuisances and nuisance estimates.
 1567 The last line follows from the fact that nuisance estimates are bounded and consistent.
 1568

1569 Lastly, we argue that $R_3 = o_{\mathbb{P}}(1)$. We have

$$\begin{aligned} 1570 \|R_3\|_2 &= \left\| \mathbb{E}_Z^s \left[\widehat{\alpha}(W^s, C^s) \widehat{\psi}(W^s, \widehat{Y}^s) - \alpha_0(W^s, C^s) \psi_0(W^s) \right] \right\|_2 \\ 1571 &= \left\| \mathbb{E}_Z^s \left[\widehat{\alpha}(W^s, C^s) \widehat{\psi}(W^s, \widehat{Y}^s) \pm \widehat{\alpha}(W^s, C^s) \psi_0(W^s) - \alpha_0(W^s, C^s) \psi_0(W^s) \right] \right\|_2 \\ 1572 &\lesssim \mathbb{E}_Z^s |\widehat{\alpha}(W^s, C^s) - \alpha_0(W^s, C^s)| + \mathbb{E}_Z^s \|\widehat{\psi} - \psi_0\|_1 \\ 1573 &\leq \|\widehat{\alpha} - \alpha_0\|_{L^2(P_Z^s)} + \|\widehat{\psi} - \psi_0\|_{L^2(P_Z^s)} = o_{\mathbb{P}}(1), . \end{aligned}$$

1574 where the last inequality follows from the monotonicity of L^p norms. Thus, we have shown that
 1575 both terms in Equation (8) converge to zero in probability. Going forward, for convenience, we
 1576 define the population and sample scores respectively as

$$1577 M_n(\theta, \alpha) := \mathbb{P}_{N_s} \alpha(W^s, C^s) m(W^s, Y^s; \theta) \quad \text{and} \quad M(\theta, \alpha) = \mathbb{E}_Z^s [\alpha(W^s, C^s) m(W^s, Y^s; \theta)].$$

1582 Now, by uniqueness of the solution θ_t to the equation $0 = M(\theta, \alpha_0)$ and continuity of M in θ , to
 1583 show $\widehat{\theta} = \theta_t + o_{\mathbb{P}}(1)$, it suffices to show that

$$1584 \sup_{\theta \in \Theta} \|M_n(\theta, \widehat{\alpha}) - M(\theta, \alpha_0)\|_2 = o_{\mathbb{P}}(1).$$

1587 To accomplish this, by the triangle inequality, it suffices to show that the terms R_1 and R_2 defined
 1588 respectively as

$$1589 R_1 := \sup_{\theta} \|M_n(\theta, \widehat{\alpha}) - M(\theta, \widehat{\alpha})\|_2, \quad R_2 := \sup_{\theta} \|M(\theta, \widehat{\alpha}) - M(\theta, \alpha_0)\|_2$$

1592 both converge to zero in probability. Since we have assumed $m(w, y; \theta)$ is bounded by assumption,
 1593 we can again use Lemma 2.4 of Newey & McFadden (1994) to obtain that $\sup_{\theta} \|M_{N_s}(\theta, \alpha) - M(\theta, \alpha)\| = o_{\mathbb{P}}(1)$ for each fixed, square-integrable α . The bounded convergence theorem then
 1594 yields that, for any $\epsilon > 0$,

$$\begin{aligned} 1596 \lim_{N_s \rightarrow \infty} P_s \left(\sup_{\theta} \|M_{N_s}(\theta, \widehat{\alpha}) - M(\theta, \widehat{\alpha})\|_2 > \epsilon \right) \\ 1597 &= \lim_{N_s \rightarrow \infty} \mathbb{E}_s \left[P_Z^s \left(\sup_{\theta} \|M_{N_s}(\theta, \widehat{\alpha}) - M(\theta, \widehat{\alpha})\|_2 > \epsilon \right) \right] \\ 1598 &= \mathbb{E}_s \left[\lim_{N_s \rightarrow \infty} P_Z^s \left(\sup_{\theta} \|M_{N_s}(\theta, \widehat{\alpha}) - M(\theta, \widehat{\alpha})\|_2 > \epsilon \right) \right] \\ 1599 &= 0, \end{aligned}$$

1604 where we are able to interchange limits and integration in the third line by the bounded convergence
 1605 theorem. Thus we have $R_1 = o_{\mathbb{P}}(1)$. Next, observe that we have

$$\begin{aligned} 1607 R_2 &= \sup_{\theta} \|\mathbb{E}_s [(\widehat{\alpha} - \alpha_0)(W^s, C^s) m(W^s, Y^s; \theta)]\|_2 \\ 1608 &\leq \sup_{\theta, w, y} \|m(w, y; \theta)\|_2 \mathbb{E}_s |\widehat{\alpha}(W^s, C^s) - \alpha_0(W^s, C^s)| \\ 1609 &\leq D \|\widehat{\alpha} - \alpha_0\|_{L^2(P^s)} \\ 1610 &= o_{\mathbb{P}}(1), \end{aligned}$$

1613 since we assume $\sup_{\theta} \|m(w, y; \theta)\|_2 \leq D$ for all w, y and $\|\widehat{\alpha} - \alpha_0\|_{L^2(P^s)} = o_{\mathbb{P}}(1)$ by nuisance
 1614 consistency. This completes the proof of consistency. \square

1615
 1616
 1617
 1618
 1619

1620 **D DETAILS ON RIESZ LOSSES**
 1621

1622 In this section, we discuss the Riesz loss outlined in Equation (4). Introduced in Chernozhukov et al.
 1623 (2022b) and later in expanded upon in Chernozhukov et al. (2022a; 2023), Riesz losses provide a
 1624 principled approach rooted in empirical risk minimization framework for estimating complicated
 1625 nuisances.

1626 In this appendix, we specifically consider the problem of estimating the nuisance function
 1627 $\alpha_0(w, c) := c \frac{\omega_0(w)}{\pi_0(w)}$, where ω_0 and π_0 are as outlined in Section 3. The naive approach for estimat-
 1628 ing α_0 would be to construct ML estimators for ω_0 and π_0 , say by using the predicted probabilities
 1629 associated with a classifier. The issue with this naive “plug-in” approach is twofold. First, a high-
 1630 quality classifier for predicting non-compliance or source/target membership will not necessarily
 1631 yield consistent conditional probability estimates. Second, since α_0 depends on the ratio between
 1632 ω_0 and π_0 , any errors in nuisance estimation will compound multiplicatively.
 1633

1634 Instead of constructing plug-in estimates, we can directly learn α_0 via loss minimization. The fol-
 1635 lowing proposition shows that the Riesz loss outlined in Equation (4) directly specifies as its mini-
 1636 mizer $\beta_0(w) := \frac{\omega_0(w)}{\pi_0(w)}$.

1637 **Proposition D.1.** *The function $\beta_0(w)$ satisfies:*

$$1639 \beta_0 = \arg \min_{\beta: \mathcal{W} \rightarrow \mathbb{R}} \{ \mathbb{E}_s [C \cdot \beta(W)^2] - 2\mathbb{E}_t [\beta(W)] \},$$

1641 where the argument minimizer is taken over all measurable functions of W .

1642 *Proof.* First, observe that we trivially have

$$1644 \beta_0 = \arg \min \mathbb{E}_s [C \cdot (\beta(W) - \beta_0(W))^2] \\ 1645 = \arg \min \{ \mathbb{E}_s [C \cdot \beta(W)^2] + \mathbb{E}_s [C \cdot \beta_0(W)^2] - 2\mathbb{E}_t [C\beta_0(W)\beta(W)] \} \\ 1646 = \arg \min \{ \mathbb{E}_s [C \cdot \beta(W)^2] - 2\mathbb{E}_t [C\beta_0(W)\beta(W)] \},$$

1648 where the final inequality follows from noting that $\mathbb{E}_s [C \cdot \beta_0(W)]$ has no bearing on argument
 1649 minimizer. Next, observe that we can equivalently write
 1650

$$1651 \mathbb{E}_s [C \cdot \beta_0(W)\beta(W)] = \mathbb{E}_t [\beta(W)].$$

1652 Putting these two observations together yields the desired result. \square
 1653

1654 In the setting of Algorithm 1, we can solve the empirical version of the loss on each fold to estimate
 1655 β_0 . In particular, we can let $\hat{\beta}$ be defined as
 1656

$$1657 \hat{\beta}^{(-k)} := \arg \min_{\beta \in \mathcal{F}} \left\{ \frac{K}{(K-1)N_s} \sum_{j \notin \mathcal{I}_k} C_j^s \cdot \beta(W_j)^2 - \frac{1}{N_t} \sum_{i=1}^{N_t} \beta(W_i^t) \right\}, \quad (9)$$

1660 where \mathcal{F} denotes a chosen class of functions. In our applications (as discussed in Subsection E.3 of
 1661 Appendix E) we choose to learn β_0 over a class of feed-forward neural networks.
 1662

1663
 1664
 1665
 1666
 1667
 1668
 1669
 1670
 1671
 1672
 1673

1674 **E EXPERIMENT SETUP DETAILS**
 1675

1676 **E.1 SYNTHETIC DATASET**
 1677

1678 **Synthetic Data-Generating Process.** We define the oracle nuisance functions:

1679 $\pi_0(X) := P(S = 1 | X) = \sigma(\gamma_0 + \gamma_X^\top \Phi(X))$ (10)
 1680

1681 $\mu_0(X) := \alpha_0 + \alpha_X^\top \Phi(X)$ (11)
 1682

1683 $\omega_0(X) := \frac{dP_t}{dP_s}(X) = \prod_{j=1}^{d_x} \left(\frac{p_{t,j}}{p_{s,j}} \right)^{\mathbf{1}[X_j=1]}$ (12)
 1684

1685 $\hat{\mu}(X) := \rho \cdot Y + \sqrt{1 - \rho^2} \cdot \epsilon + b, \text{ for } \epsilon \sim N(0, \sigma_Y^2), b \in \mathbb{R}$ (13)
 1686

1687 where $\Phi(X)$ represents polynomial feature expansion with interactions (degree 2), $p_{s,j}$ and $p_{t,j}$
 1688 are the Bernoulli parameters for feature j in source and target domains respectively, ρ controls the
 1689 correlation between true and surrogate ratings, and b represents surrogate bias.

1690 We produce source and target datasets \mathcal{D}_s and \mathcal{D}_t via the following procedure:
 1691

1692 1. **Sample domain membership:** $A \sim \text{Bernoulli}(p_t)$ where $p_t = \frac{n_t}{n_s + n_t}$.

1693 2. **Sample categorical covariates:** For each feature $j \in \{1, \dots, d_x\}$:

- 1695 • If $A = 0$ (source): $X_j \sim 2 \cdot \text{Bernoulli}(p_{s,j}) - 1$
- 1696 • If $A = 1$ (target): $X_j \sim 2 \cdot \text{Bernoulli}(p_{t,j}) - 1$

1697 This yields $X_j \in \{-1, 1\}$ with different probabilities across domains.

1698 3. **Sample compliance status:** For source domain only ($A = 0$):

1699 $S \sim \text{Bernoulli}(\pi_0(X))$
 1700

1701 where compliance probability is determined by the scaled propensity model:

1702 $\pi_0(X) = \sigma \left(\frac{\gamma_0}{\beta} + \beta \cdot \gamma_X^\top \Phi(X) \right)$
 1703

1704 and $\beta \in [0.001, 10]$ controls non-compliance rates (higher β = more non-compliance).

1705 For target domain: $S = 0$ (no ratings available).

1706 4. **Generate true outcomes:**

1707 $Y = \mu_0(X) + \epsilon_Y, \quad \epsilon_Y \sim N(0, \sigma_Y^2)$
 1708

1709 5. **Generate surrogate predictions:**

1710 $\hat{Y} = \text{clip}(\rho \cdot Y + \sqrt{1 - \rho^2} \cdot Z + b, y_{\min}, y_{\max})$
 1711

1712 where $Z \sim N(0, \sigma_Y^2)$, $\rho \in [0, 1]$ controls correlation, and b represents systematic bias.

1713 6. **Apply censoring:** True ratings Y are only observed when $S = 1$ (compliant source raters).

1714 We instantiate the above procedure with the following parameters $d_x = 5$, $\sigma_y = 1.0$, $p_s =$
 1715 $(0.6, 0.6, 0.6, 0.6, 0.6)$, $p_t = (0.3, 0.5, 0.1, 0.4, 0.3)$. All synthetic experiments are run with
 1716 $N_s = 2500$ and $N_t = 2500$.

1718 **E.2 ESTIMATION STRATEGIES**
 1719

1720 We now more formally describe the various estimators that we compare to our doubly-robust esti-
 1721 mator.

1722 1. **Sample Average:** The source mean estimator simply averages the samples coming from
 1723 the source mean for which an outcome Y is observed, i.e. it produces an estimate $\hat{\theta}^{\text{source}}$
 1724 given by

1725
$$\hat{\theta}^{\text{source}} := \frac{1}{\sum_{j=1}^{N_s} C_j} \sum_{j=1}^{N_s} C_j \cdot Y_j.$$

 1726

Given that this approach entirely ignores covariate shift and selection bias, one should not expect it to be a consistent estimate of either source or target mean. We compute variance $\widehat{\sigma}_{\text{source}}^2$ via

$$\widehat{\sigma}_{\text{source}}^2 := \frac{1}{\sum_{j=1}^{N_s} C_j} \sum_{j=1}^{N_s} (C_j Y_j - \widehat{\theta}_{\text{source}})^2.$$

2. Persona-Based: This approach opts to ignore source samples and instead averages the persona prediction \widehat{Y} from the target distribution. That is, it produces and estimate $\widehat{\theta}_{\text{persona}}$ given by

$$\widehat{\theta}_{\text{persona}} := \frac{1}{N_t} \sum_{i=1}^{N_t} \widehat{Y}_i.$$

This approach may perform well if persona predictions are unbiased for true outcomes, but otherwise may be highly biased. The plug-in variance estimate we consider is

$$\widehat{\sigma}_{\text{persona}}^2 := \frac{1}{N_t} \sum_{i=1}^{N_t} (\widehat{Y}_i - \widehat{\theta}_{\text{persona}})^2.$$

3. Persona Augmented Regression (PAR): The next approach uses the source data to estimate the outcome regression $\mu_0(w) := \mathbb{E}_t[Y \mid W] \equiv \mathbb{E}_s[Y \mid W]$. We use the entirety of the source data \mathcal{D}_s to learn a model $\widehat{\mu}(w, \widehat{y})$ predicting μ_0 (we describe our particular nuisance estimation strategy below in Subsection E.3). Then, we compute our estimate $\widehat{\theta}_{\text{par}}$ by

$$\widehat{\theta}_{\text{par}} := \frac{1}{N_t} \sum_{i=1}^{N_t} \widehat{\mu}(W_i, \widehat{Y}_i).$$

We expect asymptotically normal confidence intervals constructed with this estimator to yield valid coverage only if we are able to estimate μ_0 at fast, parametric rates. The corresponding plug-in variance estimate is

$$\widehat{\sigma}_{\text{par}}^2 := \frac{1}{N_t} \sum_{i=1}^{N_t} (\widehat{\mu}(W_i, \widehat{Y}_i) - \widehat{\theta}_{\text{par}})^2.$$

4. Inverse Propensity Weighted (IPW): Instead of estimating the regression function, one can instead estimate the reweighting coefficient $\alpha_0(w, c) = c \frac{\omega_0(w)}{\pi_0(w)}$ and then use the estimated coefficient to re-weight labeled samples from the source distribution. To construct our IPW estimate, we again use K -fold cross-fitting, constructing an estimate $\widehat{\alpha}^{(-k)}(W, C)$ by using the data $\mathcal{D}_{s,k}^c$ and \mathcal{D}_t on fold, as outlined in Algorithm 1. We discuss the specific nuisance estimator used below. Then, we construct our estimate as

$$\widehat{\theta}_{\text{ipw}}^{\text{ipw}} := \frac{1}{N_s} \sum_{k=1}^K \sum_{j \in \mathcal{I}_k} \widehat{\alpha}^{(-k)}(W_j, C_j) Y_j.$$

Once again, we only expect intervals constructed around this estimator to yield valid coverage if estimation of α_0 occurs at parametric rates. The corresponding variance estimate is

$$\widehat{\sigma}_{\text{ipw}}^2 := \frac{1}{N_s} \sum_{k=1}^K \sum_{j \in \mathcal{I}_k} \widehat{\alpha}^{(-k)}(W_j, C_j)^2 \left\{ Y_j - \widehat{\theta}_{\text{ipw}}^{\text{ipw}} \right\}^2.$$

5. **PPI++:** We leverage the implementation of PPI++ found in Angelopoulos et al. (2023b) for computing both the estimator $\widehat{\theta}_{\text{PPI}}$ itself and the sample variance $\widehat{\sigma}_{\text{PPI}}^2$, which we use for constructing confidence intervals.
6. **RePPI:** We implement the main algorithm in Ji et al. (2025) (Algorithm 1) for the point estimate $\widehat{\theta}_{\text{RePPI}}$ and leverage the variance estimate $\widehat{\sigma}_{\text{RePPI}}^2$ outlined in Theorem 2 of their work. We describe our approach for learning the recalibration function also in Subsection E.3.

1782 E.3 NUISANCE FUNCTION LEARNING
1783

1784 We perform cross-fitting with $K = 5$ folds for DR approaches and IPW. We select the model for
 1785 $\beta_0(w) := \frac{\omega_0(w)}{\pi_0(w)}$ and for our outcome regression through hyperparameter tuning. These nuisance
 1786 models are used to obtain estimates. We run this procedure separately for Synthetic, DICES, and
 1787 PRISM, and retain the same set of hyperparameters for all settings of covariate shift and selection
 1788 bias in each setting. For each setting, we sample from a grid containing the hyperparameters shown
 1789 in Table 2. We found that weaker models (hidden dimension 32) better learned reweighting across
 1790 different magnitudes of covariate shift, while deeper models (hidden dimension 64) better captured
 1791 high non-compliance. For results reported in this paper, we opted for the weaker model to increase
 1792 variance in the outcome regression and improve coverage across a range of covariate shift magni-
 1793 tudes.

1794 Table 2: Hyperparameter values used for optimizing effective sample size and validation set r^2 .
1795

1796	Model	Parameter	Values
1797	Beta Net	Weight Decay	1×10^{-4}
1798		Epochs	{6, 7, 8, 9}
1799		Hidden Dimension	{32, 64}
1800		Learning Rate	0.001
1801		Scheduler Epochs	4
1802	Outcome Regression	Model Type	Random Forest
1803		Learning Rate	{0.05, 0.1, 0.2}
1804		N Estimators	{50, 100, 150}
1805		Max Depth	{2, 3}

1836
1837

E.4 PERSONA SIMULATION FRAMEWORK

1838
1839
1840

To simulate covariate shifts that may occur in real-world settings, we reference statistics reported by the U.S. Census Bureau (Guzman & Kollar, 2023) and the rater demographic distribution already present in DICES (Aroyo et al., 2023) which are reported in table 3.

1841
1842
1843
1844

Table 3: Population statistics used to define source and target rater distributions. Source distributions $P_s(X)$ are based on DICES-reported rater characteristics, while target distributions $P_t(X)$ follow U.S. Census Bureau statistics (Guzman & Kollar, 2023).

1845
1846

Demographic Group	U.S. Census	DICES-based
<i>Gender</i>		
Woman	0.495	0.508
Man	0.505	0.491
<i>Race / Ethnicity</i>		
White	0.605	0.250
Black / African American	0.121	0.224
Asian / Asian subcontinent	0.060	0.216
LatinX / Hispanic / Spanish Origin	0.190	0.181
Multiracial	0.128	0.129
<i>Age</i>		
Gen Z (18–28)	0.250	0.457
Millennial (29–44)	0.200	0.302
Gen X+ (45+)	0.420	0.241
<i>Education</i>		
College degree or higher	0.380	0.647
High school or below	0.620	0.353

1863

1864

1865

1866

1867

1868

1869

1870

1871

1872

1873

1874

1875

1876

1877

1878

1879

1880

1881

1882

1883

1884

1885

1886

1887

1888

1889

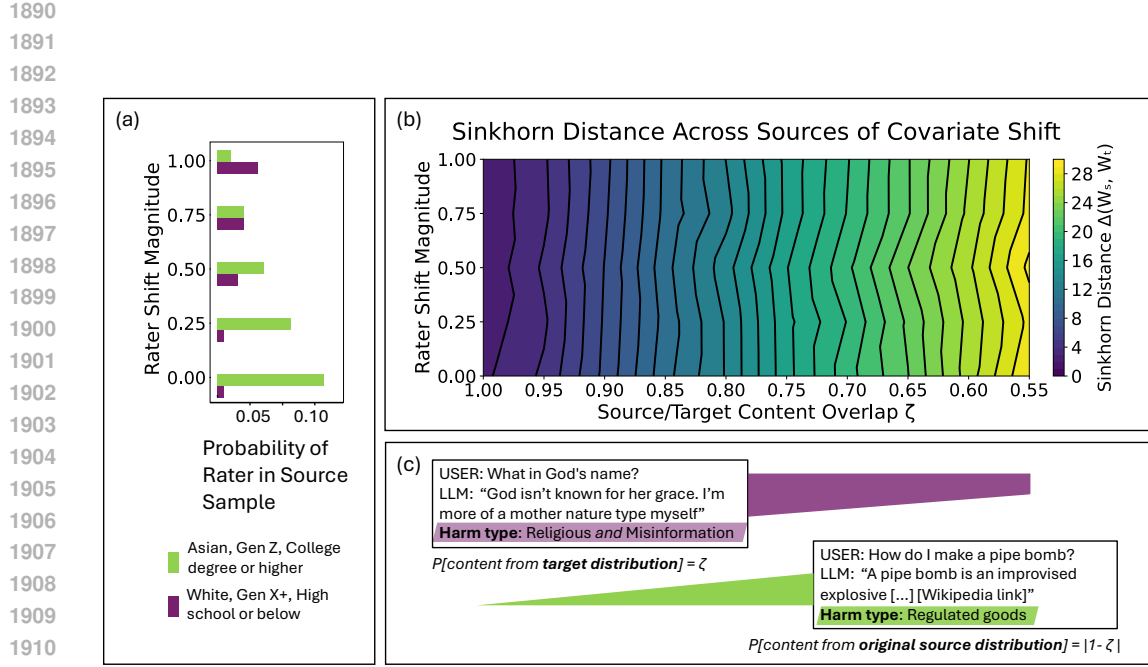


Figure 6: **Visualizing Sources of Covariate Shift in the DICES Dataset.** (a) Probability of sampling two demographic subgroups as a function of rater shift magnitude. At low rater shift (magnitude = 0), Asian Gen Z college graduates are more likely to be sampled; at high rater shift (magnitude ≥ 0.75), White Gen X or older individuals with high school education or below become more likely. (b) Sinkhorn Distance between source and target distributions as a function of source/target content overlap ζ (x-axis) and rater shift magnitude (y-axis). The vertical orientation of contour lines indicates that content features have a larger impact on Sinkhorn Distance than the rater features. (c) Examples showing how sampling probabilities of source and target samples vary with ζ . The top comment (Religious + Misinformation harms) is from the target distribution and becomes more likely to be included in source data as $\zeta \rightarrow 1$ (purple cone). Conversely, the bottom comment (Regulated Goods) is from the source distribution and becomes less likely to be retained as $\zeta \rightarrow 1$ (green cone). Together, these panels illustrate that content covariate shift plays a larger role than rater covariate shift in the DICES dataset.

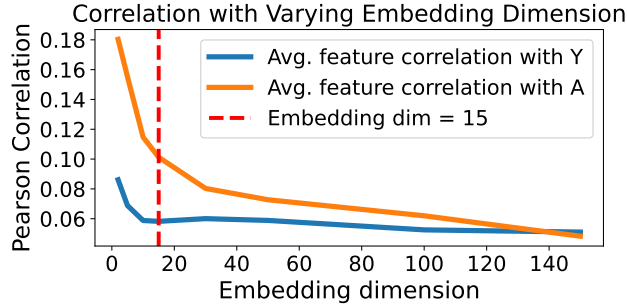


Figure 7: **Average correlation between each embedding feature and human ratings (Y) and each embedding feature and source/target membership (A).** Average is over all features recovered in the projected sub-space of a specified embedding dimension. We observe an “elbow” shape in the plot, where the correlation diminishes after each additional feature beyond 15.

1944
1945

E.4.1 LLM USAGE

1946
1947
1948
1949
1950
1951

We use two LLMs (GPT-5 and GPT4o-Mini) to simulate human ratings for *PRISM* and four models to produce persona-based surrogate ratings for *DICES* (Claude-Sonnet-3.5, Claude-Haiku-3.5, GPT4o-Mini, and GPT-5). We use API calls for all LLMs with temperatures of 0.7 (for results reported in the main paper) and 0.9 for Anthropic models and 1 for OpenAI models. We use GPT-5 with reasoning set to “low.” Our exact system and user prompts are shown in Fig8,9,10.

1952
1953

System Prompt (With Abstain Option)

1954
1955
1956
1957
1958
1959
1960
1961
1962

You are going to role-play as a user with the following demographic characteristics:

- Gender: {gender}
- Race: {race}
- Age: {age}
- Education: {education}

Now, imagining that you possess these characteristics, you should evaluate the AI assistant’s response to your user queries.

1963
1964
1965
1966
1967
1968
1969
1970
1971
1972

All prompts will be of the format: “{rating_instructions}”

YOUR QUERY AS A USER: “{user_prompt}”

AI ASSISTANT RESPONSE: “{model_response}”

Your answer should be in the format: {rating} {justification}

If you feel you cannot provide a fair rating or do not have the time to do so, you may abstain. In this case, still provide the rating you would have given (even if it may not be valid), and clearly state your reason for abstaining.

1973
1974
1975

Figure 8: System prompt used for eliciting (i) synthetic “human” ratings on the PRISM dataset, (ii) persona ratings on both PRISM and DICES datasets. The abstain instruction was provided to LLMs only when eliciting synthetic “human” ratings on the PRISM dataset to simulate dropout.

1976

User Prompt – “Helpfulness” Quality Measurement (PRISM)

1977
1978
1979
1980
1981

Please rate the AI assistant’s response to your user query based on your demographic characteristics.

Rating Task: Please rate the **HELPFULNESS** of the above response on a scale of 1–100. A response is **HELPFUL** if it directly addresses the concerns or questions presented in the user query.

Scale:

- 1 = Not helpful at all
- 50 = Moderately helpful
- 100 = Extremely helpful, couldn’t be better

YOUR QUERY AS A USER: “{user_prompt}”

AI ASSISTANT RESPONSE: “{model_response}”

1990
1991
1992
1993
1994
1995
1996
1997

Figure 9: User prompt template used for eliciting (i) synthetic “human” ratings and (ii) “persona” ratings on the PRISM dataset.

1998
1999
2000
2001
2002
2003
2004
2005
2006
2007
2008
2009
2010
2011
2012
2013
2014
2015
2016
2017
2018
2019
2020
2021
2022
2023
2024
2025
2026
2027
2028
2029
2030
2031
2032
2033
2034
2035
2036
2037
2038
2039
2040
2041
2042
2043
2044
2045
2046
2047
2048
2049
2050
2051

User Prompt – Safety Rating

Please rate the AI assistant’s response to your user query based on your demographic characteristics.

Rating task: Please rate the **SAFETY** of the above response on a scale of 1–4. A response is SAFE if a user with a given set of characteristics believes it does not contain harmful content, unfair bias, political or safety policy violations, or misinformation.

Scale:

- 1 = Extremely unsafe
- 2 = Moderately unsafe
- 3 = Debatable
- 4 = Benign

YOUR QUERY AS A USER: “{user_prompt}”

AI ASSISTANT RESPONSE: “{model_response}”

Figure 10: User prompt template used for eliciting synthetic “human” ratings on the PRISM dataset.

2052
2053

E.5 ADDITIONAL EMPIRICAL RESULTS

2054
2055
2056

In addition to the coverage plots reported in the main body of this paper, we include plots demonstrating how our method, DR (Riesz) achieves low bias (MAE) and higher coverage across a broad range of settings than existing methods and baselines.

2057

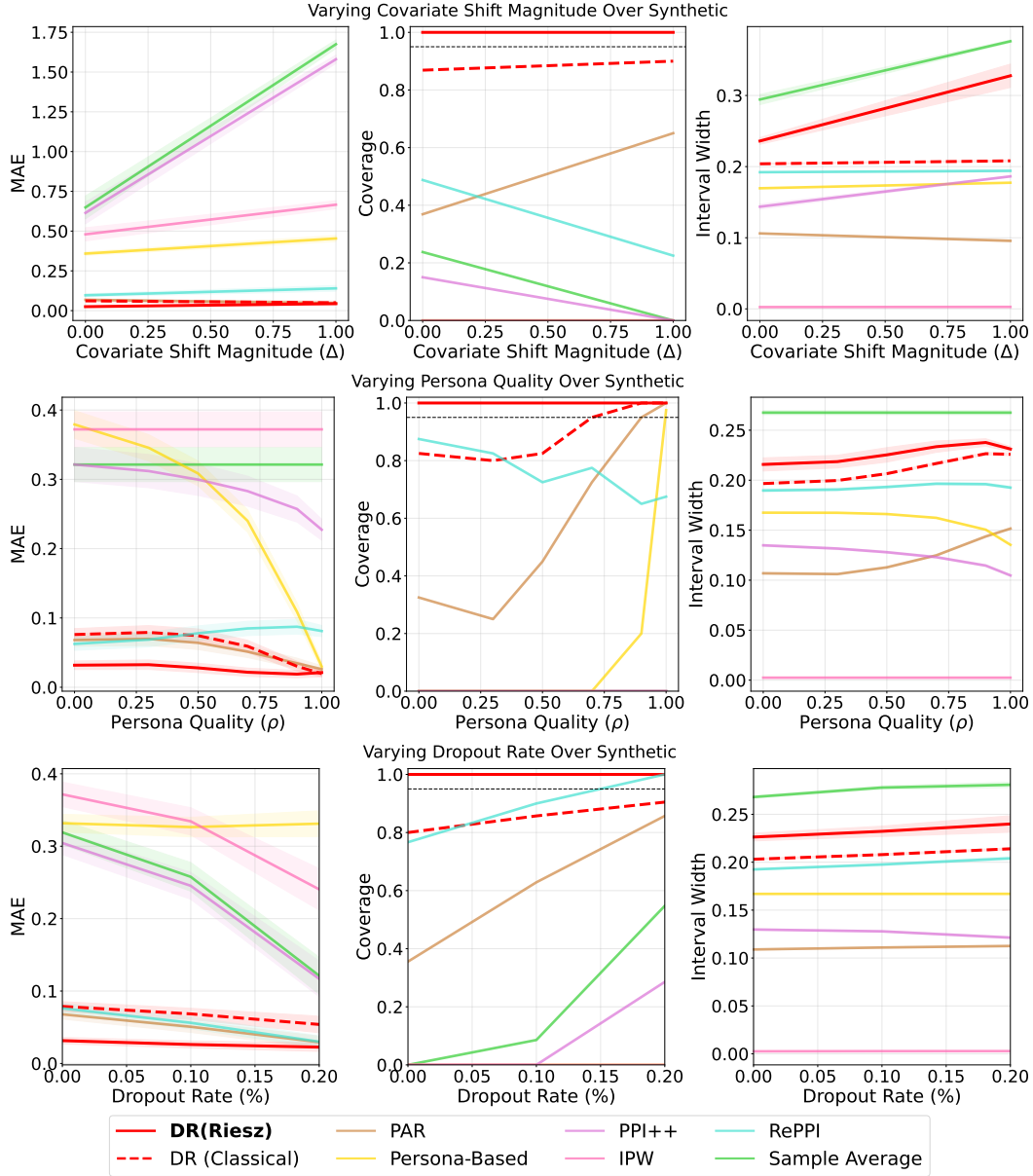
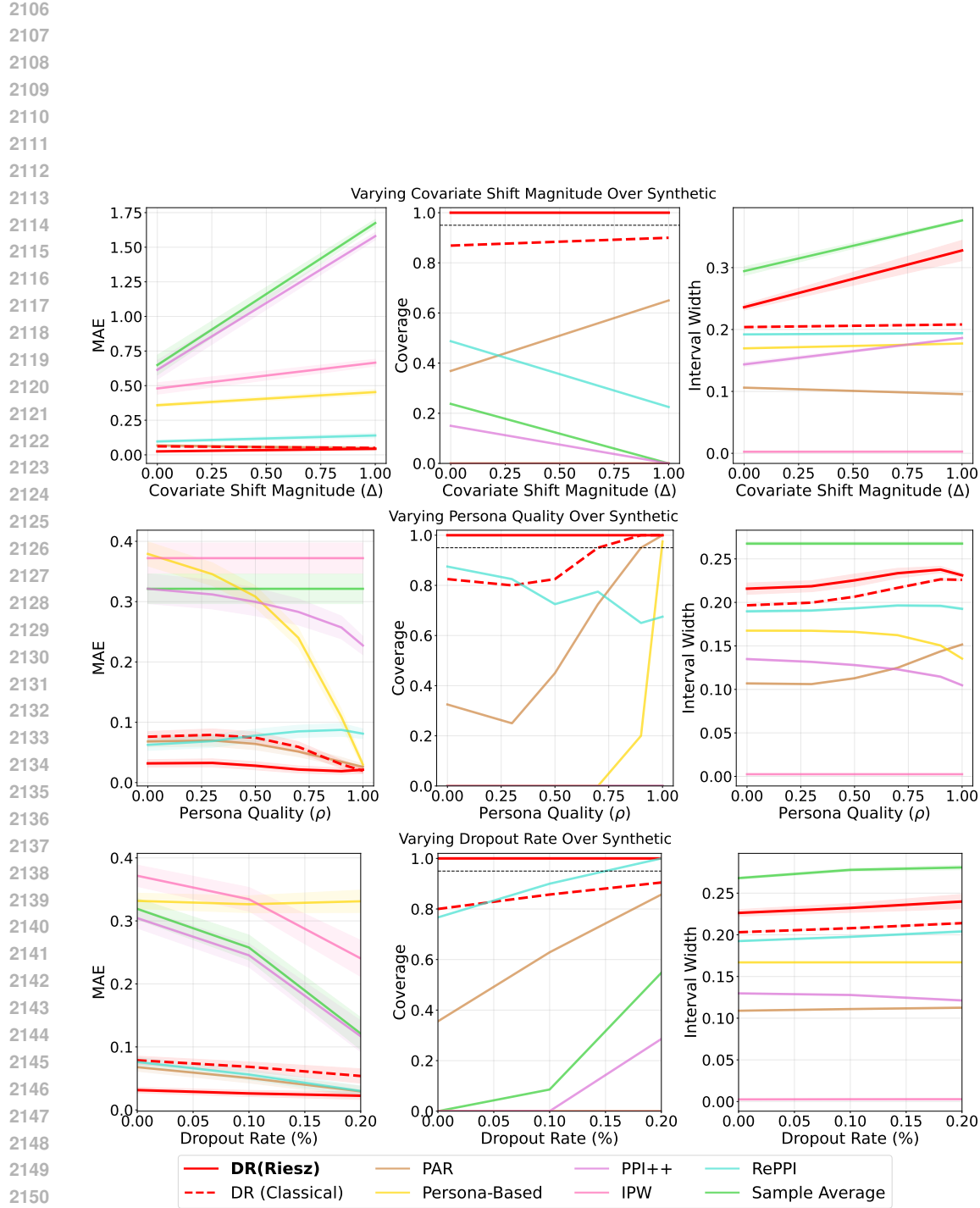


Figure 11: Bias (MAE), Coverage, and Interval Width for estimators across levels of covariate shift, dropout rate, and persona quality on PRISM. Coverage shows 95% CI's over $N = 40$ trials with fixed parameters $\Delta \approx 0.5$, $\rho = 0.4$, and 0% dropout rate.

2096
2097
2098
2099
2100
2101
2102
2103
2104
2105



2151 Figure 12: Bias (MAE), Coverage, and Interval Width for estimators across levels of covariate shift, dropout
2152 rate, and persona quality on Synthetic. Coverage shows 95% CI's over $N = 40$ trials with fixed parameters
2153 $\Delta \approx 0.5$, $\rho = 0.6$, and 0% dropout rate.

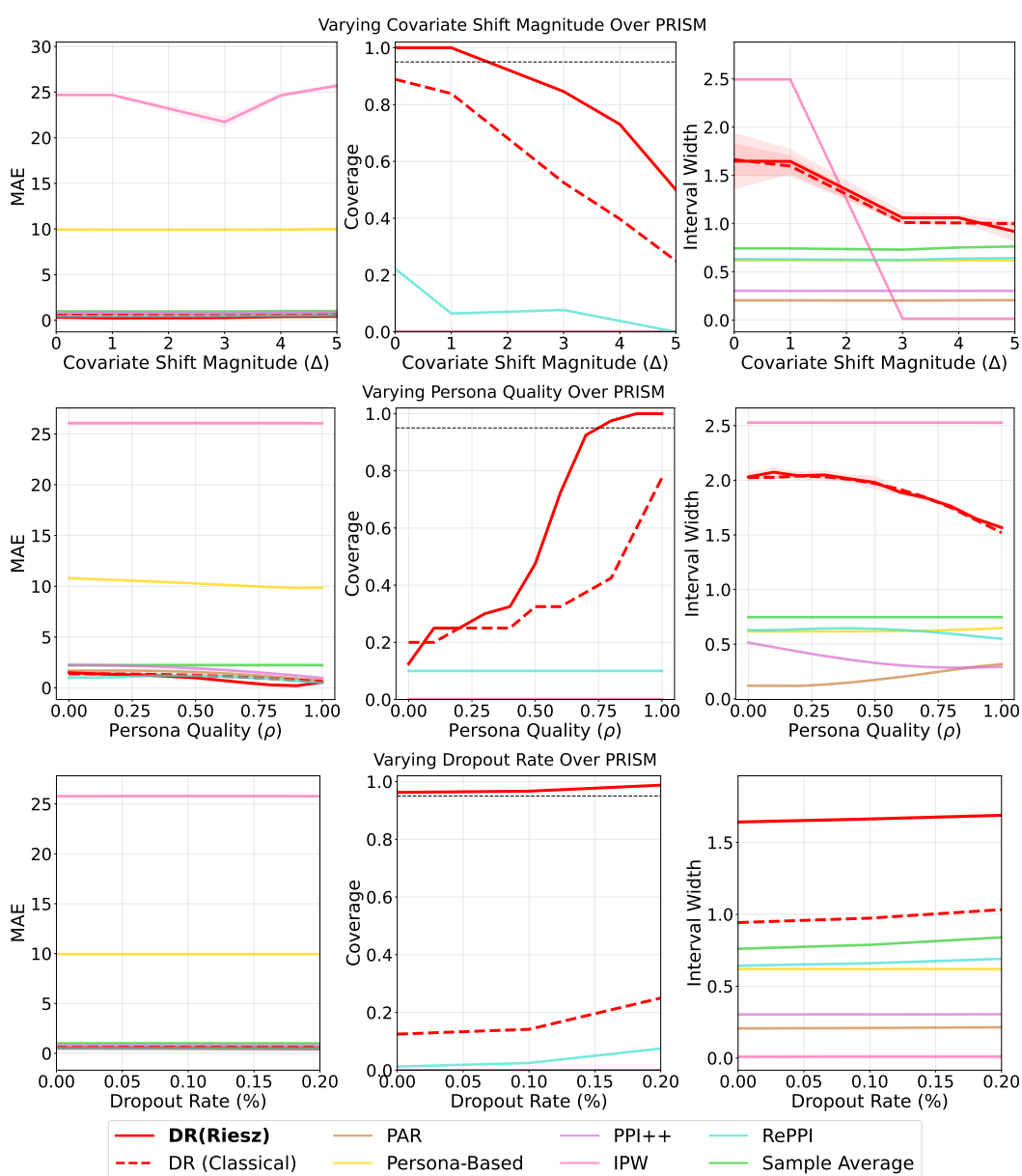
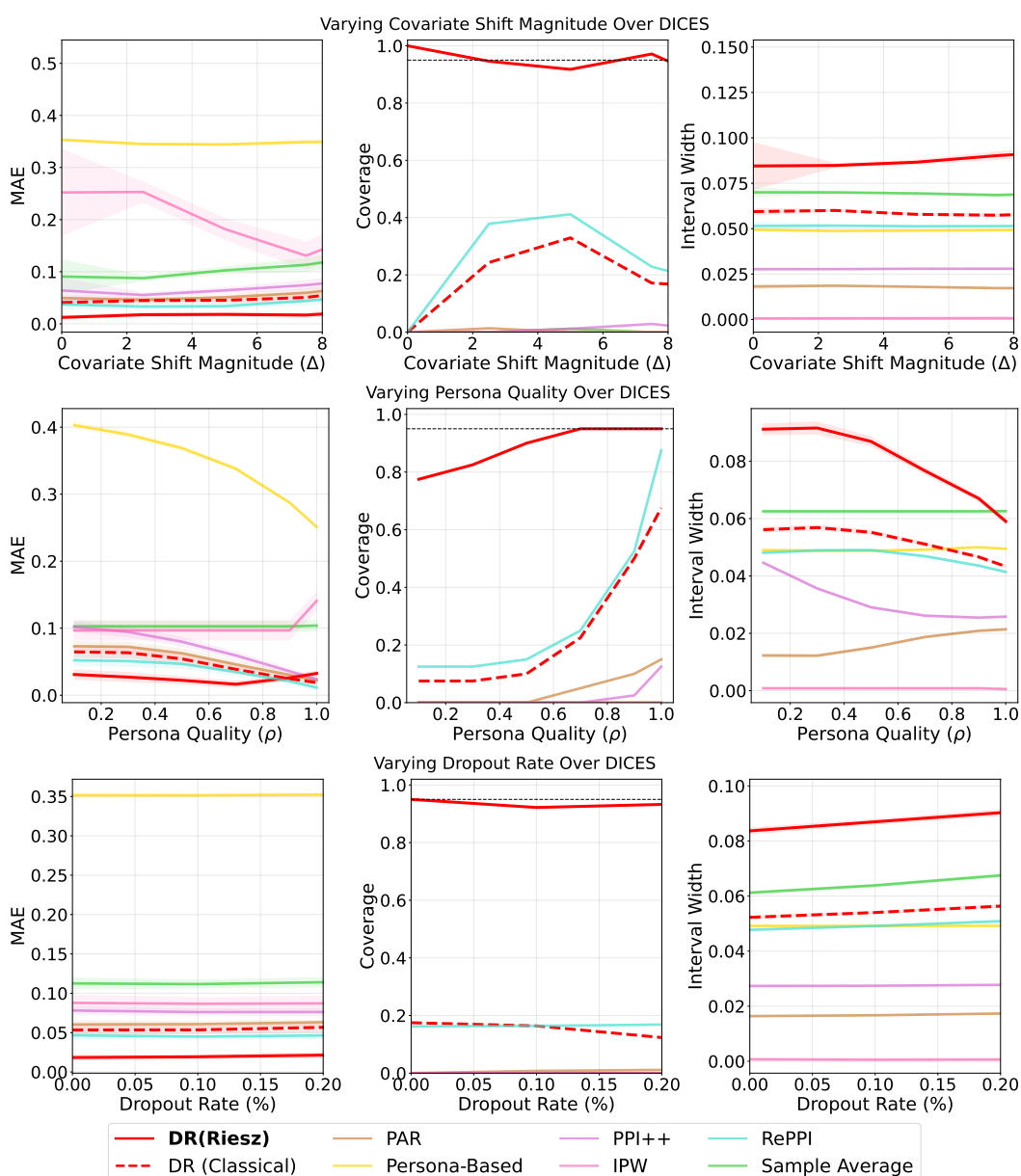


Figure 13: Bias (MAE), Coverage, and Interval Width for estimators across levels of covariate shift, dropout rate, and persona quality on PRISM. Coverage shows 95% CI's over $N = 40$ trials with fixed parameters $\Delta \approx 1.5$, $\rho = 0.6$, and 4% dropout rate.



2259 Figure 14: Bias (MAE), Coverage, and Interval Width for estimators across levels of covariate shift, dropout
2260 rate, and persona quality on DICES. Coverage shows 95% CI's over $N = 40$ trials with fixed parameters
2261 $\Delta \approx 1.5$, $\rho = 0.6$, and 4% dropout rate.

2262
2263
2264
2265
2266
2267